

# Stretched and Upside-down Maps of Auditory Space in the Optic Tectum of Blind-reared Owls; Acoustic Basis and Behavioral Correlates

Eric I. Knudsen,<sup>1</sup> Steven D. Esterly,<sup>1</sup> and Sascha du Lac<sup>2</sup>

<sup>1</sup>Department of Neurobiology, Stanford University School of Medicine, Stanford, California 94305-5401 and <sup>2</sup>Department of Physiology, University of California, San Francisco, California 94143

Vision during early life plays an important role in calibrating sound localization behavior. This study investigates the effects of visual deprivation on sound localization and on the neural representation of auditory space. Nine barn owls were raised with eyelids sutured closed; one owl was congenitally anophthalmic. Data from these birds were compared with data from owls raised with normal visual experience.

Sound localization behavior was significantly less precise in blind-reared owls than in normal owls. The scatter of localization errors was particularly large in elevation, though it was abnormally large in both dimensions. However, there was no systematic bias to the localization errors measured over a range of source locations. This indicates that the representation of auditory space is degraded in some way for blind-reared owls, but on average is properly calibrated.

The spatial tuning of auditory neurons in the optic tectum was studied in seven of the blind-reared owls to assess the effects of early visual deprivation on the neural representation of auditory space. In normal owls, units in the optic tectum are sharply tuned for sound source location and are organized systematically according to the locations of their receptive fields to form a map of auditory space. In blind-reared owls, the following auditory properties were abnormal: (1) auditory tuning for source elevation was abnormally broad, (2) the progression of the azimuths and elevations of auditory receptive fields across the tectum was erratic, and (3) in five of the seven owls, the auditory representation of elevation was systematically stretched, and in the two others large portions of the representation of elevation were flipped upside down. The following unit properties were apparently unaffected by blind rearing: (1) the sharpness of tuning for sound source azimuth, (2) the orientation of the auditory representation of azimuth, and (3) the mutual alignment of the auditory and visual receptive fields in the region of the tectum representing the area of space directly in front of the animal. The data demonstrate that the brain is capable of generating an auditory map of space without vision, but that the normal precision and topography of the map depend on visual experience.

The space map results from the tuning of tectal units for interaural intensity differences (IIDs) and interaural time differences (ITDs; Olsen et al., 1989). To explore parameters of these cues that might account for the abnormalities in the auditory space map, we measured these cues across the frontal hemifield and determined their spatial pattern (pattern of change in cue values across space), frequency dependence (variation in cue value across frequency for each location), and individual variability (variability of cue values across individuals). Comparison of these localization cue parameters with unit spatial tuning from blind-reared owls revealed the following: (1) an upside-down representation of elevation predicts an upside-down mapping of IID in the tectum—this prediction was confirmed by direct measurement of unit IID tuning; (2) the prevalence of large visual-auditory misalignments in elevation correlates strongly with the frequency dependence of IID cues produced by a sound source at the location of a unit's visual receptive field; and (3) the prevalence of large visual-auditory misalignments in azimuth correlates with the frequency dependence of both ITD and IID cues associated with the location of a unit's visual receptive field. Thus, vision is most important for the auditory representation of those peripheral locations where localization cue values are highly frequency dependent and is substantially less important for the representation of frontal locations where auditory cue values are relatively constant across frequency and predictable across individuals.

The altered topography of the auditory space map in blind-reared owls did not result from an adaptation to an abnormal motor map. The tectal map of head movement was assessed using microstimulation of physiologically defined sites. Although the topographies of both the motor map and the auditory map were abnormal, the abnormalities were different in each case and therefore represent separate effects of early blindness on the two maps.

The optic tectum (superior colliculus) contains auditory and visual maps of space that are mutually aligned: neurons in the tectum respond to auditory and visual stimuli originating from the same region of space and are organized according to the locations of their auditory and visual receptive fields to form a multimodal map of space (Gordon, 1973; Knudsen, 1982; King and Palmer, 1983; Middlebrooks and Knudsen, 1984; King and Hutchings, 1987). Because auditory spatial tuning results from neuronal selectivity for sound localization cues (such as interaural differences in time and intensity), tectal neurons must be

Received Oct. 15, 1990; revised Jan. 10, 1991; accepted Jan. 16, 1991.

We wish to thank Michael Brainard for reviewing the manuscript. This work was supported by NIH Grant R01 NS16099-10.

Correspondence should be addressed to Eric I. Knudsen, Ph.D., Department of Neurobiology, Stanford University School of Medicine, Sherman Fairchild Science Building, Stanford, CA 94305-5401.

Copyright © 1991 Society for Neuroscience 0270-6474/91/111727-21\$03.00/0

tuned for values of localization cues produced by sound sources at the locations of their visual receptive fields.

How do tectal neurons come to be tuned for the correct values of sound localization cues? Data from several species (owls, cats, ferrets, and guinea pigs) indicate that auditory spatial tuning is shaped by visual and auditory experience during development. In individuals raised with one ear occluded (which generates abnormal values of sound localization cues) or raised with displacing prisms (which shift the visual world while leaving sound localization cues unchanged), the auditory spatial tuning of tectal neurons adjusts adaptively to produce normal alignment of auditory and visual receptive fields (Knudsen, 1983, 1985; Hutchings et al., 1986; King et al., 1988). In individuals raised blind, the auditory spatial tuning of many neurons is either incorrect (i.e., not matched with the neuron's visual receptive field) or absent, implying that vision provides information essential for calibrating the auditory spatial tuning of tectal neurons (Rauschecker and Harris, 1983; Knudsen, 1988; Withington-Wray et al., 1989).

This study examines the effects of early blindness on sound localization behavior and on the auditory space map in the optic tectum of the barn owl. A previous study demonstrated that blind rearing leads to gross abnormalities in the topography of the auditory map (Knudsen, 1988). Here, we demonstrate that in different blind-reared individuals auditory maps differ dramatically, but the portions of the map that are most severely affected by visual deprivation are the same. Finally, we examine possible explanations for the differences between the portions of the map that are or are not affected by visual deprivation.

The auditory space map in the owl depends on systematic changes across the tectum in the tuning of units for binaural cues: interaural intensity differences (IIDs) and interaural time differences (ITDs; Olsen et al., 1989). The correspondence of IIDs with sound source location depends on the frequency of the sound: IIDs at lower frequencies change gradually and usually monotonically with sound source azimuth, whereas IIDs of higher frequencies change rapidly and nonmonotonically with both the azimuth and elevation of the source (Olsen et al., 1989). (In barn owls, an asymmetry in the external ears produces a strong elevational dependence of IIDs for frequencies above 3 kHz, providing the owl with IID cues that are sensitive indicators of sound source elevation.) The correspondence of ITDs with source location also depends on frequency because of the frequency-dependent effect of the head and ears on sound propagation (Kuhn, 1977; Roth et al., 1980; Olsen et al., 1989). Consequently, for most locations the values of sound localization cues produced by a sound source vary with frequency, and the neurons in the space map are tuned for these frequency-dependent variations in IID and ITD (Esterly and Knudsen, 1989). In addition, the IIDs and ITDs corresponding with a given region of space can differ across individuals because of differences in the size and shape of the head and ears. Here, we analyze the frequency dependence and individual variability of IID and ITD spectra measured throughout the frontal hemifield, and relate these values to the prevalence of auditory spatial tuning errors for corresponding locations in the map. The results support the hypothesis that the portions of the map that must interpret complex (frequency-dependent) spectra are particularly dependent upon visual experience.

At the outset of these experiments, it was not known whether the degradation in auditory spatial tuning that results from blind rearing is due to the loss of a direct influence of vision on the

auditory map, or whether it is caused secondarily by the degradation of the motor map that also occurs as a consequence of blind rearing (du Lac and Knudsen, in press). The motor map is a topographic representation of the size and direction of orienting movements that are specified by tectal output. In normal animals, the motor map is aligned with the visual and auditory maps: the movement elicited by electrical stimulation of any given site in the tectum brings the animal's gaze to the point in space that was at the center of the sensory receptive fields at that site prior to the movement (Sparks, 1986; du Lac and Knudsen, 1990). In blind-reared owls, electrically evoked movements tend to be too small, too large, and/or inaccurately directed compared with the movements predicted by the locations of visual receptive fields (du Lac and Knudsen, in press). Data presented in this report demonstrate that the auditory and motor maps are degraded in different ways as a consequence of blind rearing, indicating that the abnormal topography of the auditory map does not result from abnormal topography of the motor map.

## Materials and Methods

This study is based on data from 21 barn owls (*Tyto alba*): 10 were raised blind, and 11 were raised with normal sight; one blind-reared owl was congenitally anophthalmic. Electrophysiological recordings were made in seven blind-reared and three normal owls; four of these blind-reared owls were also used in electrical microstimulation experiments. Interaural difference spectra were measured in five additional normal owls. Behavioral experiments testing sound localization accuracy were carried out on three additional blind-reared and three additional normal owls. Some of the electrophysiological data from four owls (blind-reared owls 1–3 and normal owl 8) have appeared previously (Knudsen, 1988).

**Experimental manipulation.** Eyelids were sutured closed at 10–13 d of age, when the eyelids normally begin to open. At this age, the ocular medium is cloudy, the eyes have not yet assumed adult orientations, and there is no behavioral evidence of spatial resolution (Knudsen, 1989). The owllets were anesthetized with halothane and nitrous oxide, and the margins of the lids were incised and sutured together. Within days, the upper and lower lids fused to form continuous dermal layers covering the eyes.

Eyelids were opened at various ages ranging from 2 to 6 months. At the time the eyelids were opened, a head plate to fix the head in a stereotaxic device (for physiology) or to hold a search coil (for behavior) was cemented to the skull. Owls studied electrophysiologically also had removable opaque occluders mounted over the eyes to prevent vision between recording experiments. Owls studied behaviorally were without optical obstruction from the day of eyelid opening onward. After the eyelids were opened, the eyes were treated daily with ophthalmic antibiotic (bacitracin–neomycin–polymyxin) until the wounds healed.

**Spatial coordinates.** All angles and directions are defined according to a head-centered coordinate frame: azimuth (Az) indicates degrees left (L) or right (R) of the owl's midsagittal plane; elevation (El) indicates degrees above (+) or below (–) the owl's visual plane, all angles being measured from the intersection of the interaural axis with the midsagittal plane. The properties of this double-pole coordinate system are discussed in detail in a previous report (Knudsen, 1982).

**Electrophysiological analyses.** Physiological experiments were conducted in a sound isolation chamber (IAC 404A) lined with acoustic foam wedges to suppress echoes. Free-field auditory stimuli were presented from a dynamic loudspeaker that moved by remote control on a semicircular track (radius, 92 cm). The track itself rotated, allowing the experimenter to position the sound source at nearly any location on a sphere centered on the owl's head.

Experiments were carried out while the animals were anesthetized with intramuscular injections of ketamine HCl (15 mg/kg) and diazepam (5 mg/kg). The anesthetized bird was wrapped in a leather jacket, and the head was bolted to a stereotaxic device using the threaded plate that was cemented to the skull. The heads of normal owls were positioned using retinal landmarks (superior tips of the pecten oculi) to align the visual axes with the speaker-moving system (Fig. 1); the eyes in adults are essentially immobile in the head. As expected from a previous study (Knudsen, 1989), the eyes of nearly all blind-reared owls were oriented

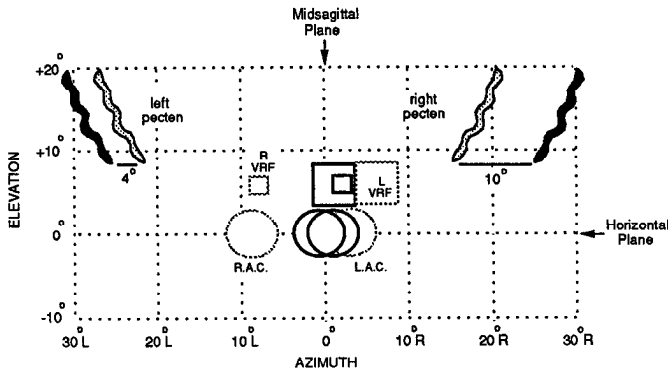


**Figure 1.** Correction of visual receptive field (VRF) locations for abnormal eye positions. Because the locations of visual receptive fields are reported in head-centered coordinates, measured locations had to be adjusted for abnormal eye positions in owls with strabismus (Table 1). These data are from a unit recorded in owl 1, which was cross-eyed. The left-eye and right-eye receptive fields that were actually measured are indicated by the dash-outlined squares. Adjusting the receptive field locations by the differences between the measured positions of the pecten (shaded) and the mean positions of the pecten measured in normal owls (solid) causes the left-eye and right-eye receptive fields to become mutually aligned (solid-outlined squares). This correction also brings the visual axis of each eye (left and right areae central; L.A.C. and R.A.C., respectively) into a normal orientation relative to the head.

abnormally (Table 1). Consequently, the heads of blind-reared owls were positioned according to planes defined by the facial lore feathers and the angle of the beak so that these planes matched those of normal owls in the standard position. This technique aligned the head correctly to within 1° Az and 3° El based on measurements in normal owls.

Units and unit clusters were recorded extracellularly with insulated tungsten microelectrodes or glass micropipettes. Electrodes were positioned stereotactically and passed through the telencephalon for about 1.2 cm before reaching the optic tectum. The appearance of bursting unit activity signaled the entrance of the electrode into the superficial layers of the tectum (Knudsen, 1982).

Auditory spatial tuning was measured using broadband noise bursts from the free-field loudspeaker. Noise bursts were 50 msec in duration, 20 dB above the unit's threshold, and presented once per second. Responses to eight repetitions of the noise burst were collected at 5° or 10° intervals in azimuth and elevation across the unit's receptive field. A unit's best area was defined as the area of space from which the stimulus elicited >50% of the maximum number of action potentials. The size of a best area indicates breadth of spatial tuning; the center of a best area represents the location of spatial tuning. Frequency tuning was measured with the loudspeaker positioned at the best-area center. The characteristic frequency (CF), the frequency to which a unit is most sensitive, was measured by sweeping a range of frequencies (using tone bursts with 5-msec rise and fall times) while slowly increasing the sound level and listening for stimulus-locked responses. Sharpness of frequency tuning was expressed as  $Q_{10dB}$  values, defined as a unit's CF divided by the range of frequencies to which the unit responded at 10 dB above threshold with stimulus-locked spikes.

Unit tuning for ITD and IID was measured by presenting noise-burst stimuli through earphones. The dichotic stimuli consisted of computer-generated, 4-kHz high-pass noise transduced by subminiature earphones (Knowles ED-1914) coupled to damping assemblies (Knowles BF-1743). The earphones were calibrated and positioned in the ears as described previously (Olsen et al., 1989). The frequency response of each earphone was flat to within 2 dB from 4 to 10 kHz. The amplitude of the signal for each channel was controlled with a programmable attenuator. Time delays between the channels were produced by computer-calculated shifts in the waveform of the signal (Olsen et al., 1989). For each measurement, 10 series of stimuli were presented at a rate of 1/sec at an average binaural intensity of 20 dB above threshold. Within each series, the order of ITD or IID values was randomized. When ITD tuning was measured, IID was held constant at its best value; when IID tuning was measured, ITD was held constant at its best value. Best values were defined as the center of the range of values for which a stimulus produced

**Table 1.** Eye orientations of owls in physiological study

Owl	Left eye (degrees left)		Right eye (degrees right)	
	Projection <sup>a</sup>	Correction <sup>b</sup>	Projection <sup>a</sup>	Correction <sup>b</sup>
<b>Blind-reared</b>				
1	22	+4	16	+10
2	29	-3	30	-4
3	28	-2	29	-3
4	22	+4	23	+3
5	26	0	26	0
6	23	+3	23	+3
7	19	+7	18	+8
<b>Normal</b>				
8	25		25	
9	26		26	
10	26		26	

<sup>a</sup> Projection of the superior tip of the pecten oculus.

<sup>b</sup> Correction to mean normal eye orientation of 26°.

>50% of the maximum number of action potentials.

Sites of recording in the tectum were estimated on the basis of visual receptive field locations (corrected for abnormal eye orientation; see below). A unit's visual receptive field was defined as the area from which stimuli produced an increase in discharge rate. Visual stimuli consisted of bars and spots from a hand-held projector, imaged on a translucent hemisphere (radius, 57 cm) that was brought into the chamber for visual tests and then was removed. The hemisphere was aligned and calibrated with the coordinate system defined by the speaker-moving system.

**Correction of visual receptive fields for abnormal eye orientation.** Because we used a head-centered (rather than eye-centered) coordinate system to define visual and auditory spatial tuning, the locations of visual receptive fields measured in blind-reared owls had to be corrected for abnormal eye position (Table 1). In normal owls, eye orientation in the orbit is essentially constant: with the head in standard position, the projection of the superior tip of the pecten oculus ranges from 24° to 27° Az (median, 26°;  $n = 40$ ) and from +5° to +11° El (median, 8°; Knudsen, 1989). The eye orientations of the normal owls in this study fell within these ranges. In the blind-reared owls, the eyes were oriented approximately normally in the vertical plane, but were exotropic in owls 2 and 3 and esotropic in owls 1, 4, 6, and 7; Figure 1 shows the esotropic (crossed) orientation of the eyes of owl 1. In normal birds, most units in the region of the tectum that represents the binocular visual field have binocular receptive fields, and the left-eye and right-eye receptive fields align to within a few degrees (Knudsen, 1989). In the blind-reared owls with abnormal eye orientations, most units in this region of the tectum had binocular receptive fields, but the left-eye and right-eye receptive fields were misaligned in azimuth. As shown in Figure 1, the receptive field misalignment corresponded to the deviation in the orientation of the eyes from normal. Adjusting the azimuthal position of each receptive field (Fig. 1, dash-outlined squares) by the difference between normal eye orientation (26°) and actual eye orientation usually brought the left-eye and right-eye receptive fields into the normal range of alignment (Fig. 1, solid-outlined squares) and brought the mean binocular misalignment for all units in each bird to approximately 0° (Knudsen, 1989).

The locations of all visual receptive fields reported in this study have been corrected for the abnormal eye positions listed in Table 1. After correcting for eye position, the centers of left-eye and right-eye receptive fields sometimes still differed by as much as 5° (slightly beyond the range of receptive field disparities observed in normal owls; Knudsen, 1989). Whenever there was any residual disparity between monocular receptive fields, the visual receptive field location reported is that measured for the dominant, contralateral eye.

**Histological reconstruction of recording sites.** In the final experiment on owls 1 and 3, electrolytic lesions were placed at the sites of the first and last units in each of a total of eight penetrations. After 2 d, the owls were anesthetized deeply with pentobarbital sodium and perfused through the heart with 0.1 M phosphate buffer, followed by formalin. The head

was mounted in the stereotaxic frame, and the brain was blocked in the transverse plane, parallel to the electrode tracks. Frozen sections were cut at 30  $\mu\text{m}$ , and every third section was mounted and stained with cresyl violet.

Lesions were matched with corresponding electrode penetrations. The positions of 30 recording sites were reconstructed from depths, measured by the microdrive, relative to the top and bottom lesions. Reconstructed recording sites were entered on brain atlas sections made from identically processed tissue from normal owls (Knudsen, 1982). The intervals between atlas sections were 180  $\mu\text{m}$ , which limited the precision of positioning recording sites to approximately 100  $\mu\text{m}$  in the rostrocaudal dimension. The atlas sections, with reconstructed recording sites, were transformed into a flattened projection (Knudsen, 1982). The flattening procedure normalized all tectal layers to the dimensions of the stratum opticum. Hence, comparisons between tectal maps refer to distances along this outermost layer.

**Interaural difference spectra.** In five owls, we measured the interaural differences in the timing and intensity of sound for sources located at 10° intervals in azimuth and elevation across the entire frontal hemifield. Broadband noise presented from the movable loudspeaker was recorded from each ear canal with probe tube microphones (length, 35 mm; internal diameter, 0.5 mm; coupled to 1/2-inch Bruel and Kjaer #4133 condenser microphones) positioned as described by Olsen et al. (1989). Interaural difference spectra for phase and intensity, corrected for differences between the probe tubes, were calculated at 25-Hz intervals using a fast Fourier transform spectrum analyzer. ITD spectra were calculated from interaural phase-difference spectra by converting phase differences to time differences at the low-frequency end of the spectrum, where the interpretation of phase differences is not ambiguous. The time values for lower frequencies were used to resolve phase ambiguities at higher frequencies by selecting the minimum change in ITD value with frequency whenever ITD changed with frequency. Contour plots of ITD and IID values were generated on a VAX-VMS workstation using software obtained from S. Guilloateau, Institut de Radio Astronomie Millimétrique, 300 Rue de la Piscine, F-38406 Saint Martin d'Herès, CEDEX, France.

Three properties of the ITD and IID spectra were analyzed: (1) The *spatial patterns* of ITD and IID values were plotted from averaged values from five normal owls, using data for a 1/3-octave band from 6.3 to 8.0 kHz. (2) The *frequency dependence* of ITD and IID was calculated for each location as the standard deviation of ITD or IID values in a frequency band from 3 to 9 kHz. The standard deviations from the five birds were averaged to yield a mean standard deviation for the spectra from each of the source locations. (3) The *individual variability* of ITD and IID spectra was calculated for each source location as the standard deviation of the ITD or IID values from the five birds at each frequency, and these standard deviations were then averaged across frequency from 3 to 9 kHz.

**Inference of unit tuning from spatial patterns of cues.** Only in a few cases was the IID and ITD tuning of units measured directly using dichotic sound presented through earphones. For the vast majority of the units, tuning for IID and ITD over a 1/3-octave interval centered at 7 kHz (IID<sub>7kHz</sub> and ITD<sub>7kHz</sub>, respectively) was estimated from the cue values associated with the location of the best-area center, as derived from contour plots of cue spatial patterns (averaged over the 1/3 octave from 6.3 to 8.0 kHz; see Fig. 8). The IID<sub>7kHz</sub> and ITD<sub>7kHz</sub> values to which a unit would be expected to be tuned if it had no alignment error were estimated from the cue values corresponding to the location of the unit's visual receptive field. These estimates assume (1) that a unit's spatial tuning was dominated by its cue tuning in this frequency range (this range is the best approximation, based on data from normal owls; Olsen et al., 1989), and (2) that the values from the averaged interaural difference spectra were close to those for the respective individual (see Fig. 13C,D for quantitative evaluation). These assumptions should be kept in mind whenever we use unit spatial tuning to infer tuning to localization cue values. In the few cases ( $n = 17$ ) where tuning to interaural differences was measured directly (e.g., Fig. 10), the measured IID tuning matched the inferred IID<sub>7kHz</sub> tuning to within 3 dB with two exceptions, and the measured ITD tuning matched the inferred ITD<sub>7kHz</sub> tuning to within 25  $\mu\text{sec}$  with one exception.

**Analysis of stimulation-evoked movements.** The movements encoded by output from restricted portions of the tectum were determined using electrical microstimulation in awake birds. Insulated tungsten electrodes, 0.2–0.8 M $\Omega$  (at 1 kHz), were positioned in the tectum and were cemented in place with dental acrylic. Auditory and visual receptive fields were measured as described above, and the owl was returned to

its holding cage to recover from the anesthetic. After 24–48 hr, the alert owl was placed in a padded restraining tube that allowed the head to move freely. Electrical stimulation consisted of 500- $\mu\text{sec}$  cathodal pulses delivered at 500 Hz for 80 msec with current strengths ranging from 200 to 800  $\mu\text{A}$ . Head movements were monitored with a search coil system (C-N-C Engineering). The search coil was accurate to within 1° over the range that measurements were taken. Head movement data were recorded on magnetic tape and were digitized (500-Hz sampling rate) and analyzed off line.

For each stimulation site, the size and direction of the movement vector that was characteristic of that site were determined by starting every trial with the head straight on the body and increasing the current strength with each trial until the size of the movement plateaued. Movement vectors evoked with these current levels were reproducible, varying by 0.8–3.6° (SD). The mean vector from eight or more movements is reported as the *characteristic vector* for that stimulation site (du Lac and Knudsen, 1990).

After completing the electrical stimulation experiments (which required 3–7 d), visual receptive fields were measured again to determine whether the electrodes had moved over the course of electrical stimulation. Electrode position was always found to be unchanged. However, in several cases electrode quality had deteriorated, and the stimulation data from these sites were discarded.

**Behavioral analysis.** Normal owls ( $n = 3$ ) were trained to stand on a small perch and to orient the head toward auditory and visual stimuli to receive a food reward. The tests were carried out in a darkened sound chamber. Auditory stimuli consisted of repetitive noise bursts of variable amplitude, duration, and repetition rate generated by the free-field speaker. Visual stimuli consisted of a modulated glow from a light-emitting diode (LED) that was centered in the speaker cone and traveled with the speaker. Head orientations were monitored using a head-mounted search coil. Tests were conducted in the following manner: the lights in the sound chamber were extinguished, and the loudspeaker/LED was moved to a random location in front of the owl. Then, either the auditory or the visual stimulus was presented until the owl made an orienting response, after which the owl received a food reward. The loudspeaker/LED was then moved to a new, random location. Although stimulus locations were selected at random, no location was greater than 30° from the starting head position. Within this area, normal barn owls are uniformly accurate and precise at localizing auditory and visual stimuli (Knudsen et al., 1979). The orientation of the search coil relative to the head was determined from the mean response for all orientations to the visual stimulus (collected after eyelid opening in the blind-reared birds).

Eyeid-sutured owls ( $n = 2$ ) were trained with the eyelids still closed, using the same techniques but without visual stimuli. These birds were more difficult to train. They tended to hold the head in odd positions between trials, and their orientation movements tended to be slower, though each bird generated kinetically normal head saccades on occasion. Once each owl was performing the behavioral paradigm reliably, it was tested in three to five consecutive sessions, each session involving 15–25 responses to the sound source. Mean response errors indicate average localization accuracy for sources located within 30° of straight ahead. The scatter of the individual responses around the mean values reflects both general imprecision in localization and any location-specific, systematic errors in localization.

After orientation responses to the auditory stimulus had been collected, the eyelids of the blind-reared owls were opened, and responses to visual stimuli were measured; the owls oriented to visual stimuli on the first day after eyelid opening. The anophthalmic owl (Table 2, Dy), which came to us as an adult, was not trained. Nevertheless, it made saccadic orienting head movements toward the noise source, and these were used to estimate sound localization.

## Results

### *Sensory experience and sound localization*

Blind and normal-sighted owls were raised in communal aviaries. By about 14 d of age, the owls oriented the head in response to novel sounds. Head orientations to visual stimuli began 3 or 4 d later in the sighted birds. Blind and sighted owls interacted with equal vigor and engaged in grooming and chasing, with physical contact between owls often accompanied by vocalizations. As the owls matured, they began pouncing on small ob-

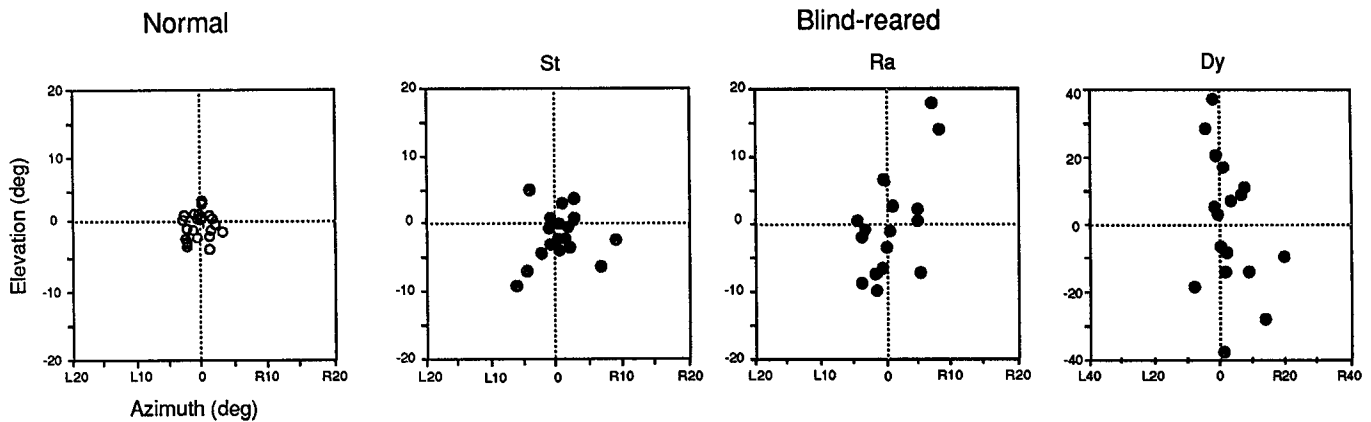


**Figure 2.** Head orientations to auditory stimuli by one normal and three blind-reared owls. Individual responses, gathered in single test sessions for each bird, are plotted in coordinates of space relative to the location of the sound source. The data are from *normal owl Am* (open circles), and blind-reared owls *St*, *Ra*, and *Dy* (solid circles). Note the change in scale for the data from *Dy*. The absolute values of the data from *Dy* are arbitrary, because visual responses could not be obtained from this anophthalmic bird to determine search coil orientation on the head; the raw values from the search coil minus the coordinates of the sound source are plotted.

jects (sighted birds) or without apparent targets (both blind and sighted owls). By 6 weeks of age, all of the birds made crisp, rapid head movements toward novel stimuli.

The behavior of sighted and blind birds became clearly discrepant by 8 weeks of age. Sighted birds began to fly and to explore the aviary aggressively. Blind birds were less active and tended to remain on a perch or on the floor. Several of them adopted abnormal resting head postures, tilting the head upward, downward, or to the side when standing undisturbed.

Orientation movements made by blind-reared owls were always in the approximate direction of the sound source. Mean orientation errors, calculated for each test session, ranged from L2.7° to R1.1° Az and from -3.7° to +0.9° El for owl *St*, and from R0.2° to R3.2° Az and from -2.5° to +3.9° El for owl *Ra* (mean error could not be determined for the anophthalmic owl *Dy* because visual responses could not be obtained to calibrate search coil orientation). These values were not different from those observed in the normal owls (Table 2). Thus, sound localization by the blind-reared owls was not systematically biased in any particular direction. However, the distribution of errors by blind-reared owls was abnormally broad (Fig. 2), as shown by the SD of the orientation errors (Table 2). Although each blind-reared owl was more precise at localizing sound sources in azimuth than it was at localizing sources in elevation, the SDs in both dimensions were significantly worse than in normals ( $p < 0.01$ ,  $F$  test).

The two eyelid-sutured owls (*St* and *Ra*) were also tested for localization of visual targets over a period of days immediately following eyelid opening. In both cases, though SDs for visual localization [*St*, 2.8° Az, 3.0° El; *Ra*, 2.7° Az, 2.9° El] were larger than those measured from any of the normal owls (1.6–2.1° Az, 1.5–2.6° El), none were significantly different at the  $p < 0.05$  level ( $F$  test). Thus, deterioration of head motor control was not responsible for the dramatic decrease in the precision of orientation responses to sound sources that was observed in the blind-reared owls.

#### General observations about unit properties

Neural activity was abnormal in the tecta of blind-reared owls. Spontaneous activity tended to be low, particularly in the superficial layers (layers 1–10). Regions of physiologically inactive

tissue were encountered occasionally throughout the tectum. Although background hash responded strongly and repeatedly to visual (superficial layers) or to auditory (deep layers) stimuli, unit responses tended to be sluggish and to habituate. Sustained responses outlasting the stimulus, typical in normal birds (Knudsen, 1984), were rarely observed. In the superficial layers, where nearly all bursting units are normally bimodal, many bursting units responded well only to one modality and poorly or not at all to the other. Some spontaneously active units could not be driven by either modality. Sizes of visual receptive fields (median width, 3.2°; range, 0.5–23°;  $n = 334$ ) were generally smaller than in normal birds (median, 5.5°; range, 0.5–40°;  $n = 127$ ). This was due in part to erratic or habituating responses in blind-reared birds to stimuli presented near the edges of receptive fields; visual receptive fields reported here represent only the region where stimuli elicited a reliable response.

The electrophysiological data presented in the following sections represent a somewhat biased account of the effects of blind rearing on unit response properties, because units that did not respond to the acoustic search stimulus were not usually studied.

**Table 2.** Sound localization by blind-reared and normal owls

Owl	Mean response error <sup>a</sup>		SD <sup>b</sup>	
	Azimuth (in degrees)	Elevation (in degrees)	Azimuth (in degrees)	Elevation (in degrees)
<b>Blind-reared</b>				
<i>St</i>	L2.1	-2.9	3.6**	4.5**
<i>Ra</i>	R1.8	+3.2	4.0**	9.5**
<i>Dy</i>	—	—	5.7**	15.7**
<b>Normal</b>				
<i>Ka</i>	R1.1	-1.7	2.1	2.0
<i>Am</i>	L2.2	-2.9	2.0	2.5
<i>PI</i>	L1.6	+0.3	1.8	2.7

<sup>a</sup> Median of the mean signed response errors measured in three to five test sessions. Sample size for each test session ranged from 15 to 25.

<sup>b</sup> Median of the SDs of response errors measured in three to five test sessions.

\*\* Significantly different from normal at the  $p < 0.01$  level ( $F$  test).

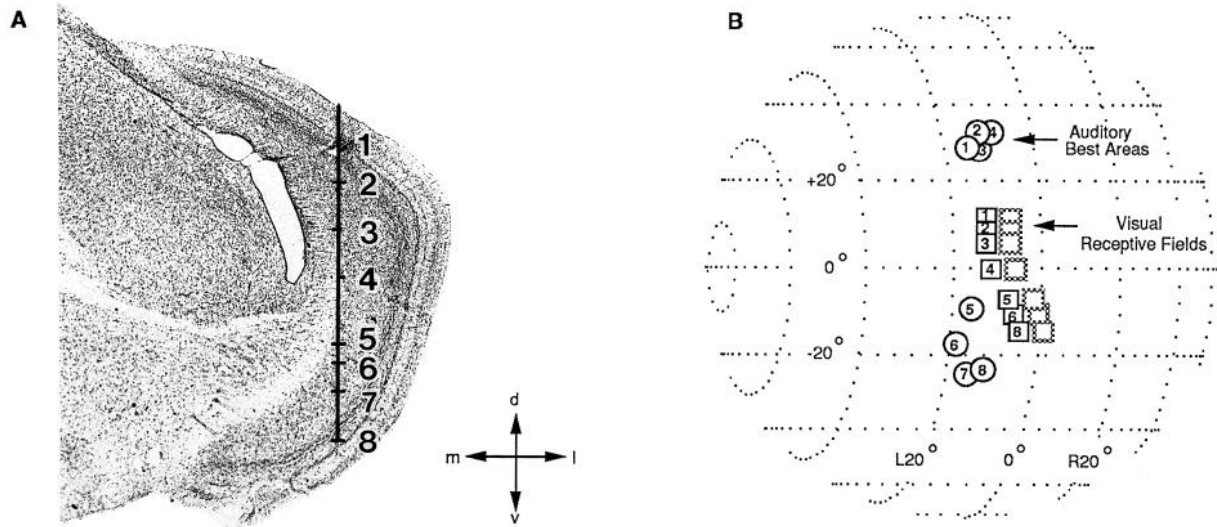


**Figure 3.** Reconstruction of an electrode track through the right optic tectum of blind-reared owl 1. *A* is a Nissl-stained, transverse section of the tectum showing the trajectory of the electrode and the locations of eight recording sites. The scale, below and to the right, indicates the orientation (*d*, dorsal; *l*, lateral) and the magnification (arrowhead to arrowhead, 1 mm) of the section. *B* shows the plots of the centers of auditory best areas (circles), measured visual receptive field centers for the contralateral (dominant) eye (stipple-outlined squares), and visual receptive field centers corrected for strabismus (solid-outlined squares), plotted in head-centered coordinates of space. The numbers correspond with the recording sites in *A* from which the data were collected. The unit recorded at site 7 did not respond to visual stimulation.

This report focuses primarily on the subset of units and unit clusters that could be driven both by visual and by auditory stimulation.

#### Visual receptive field location as an anatomical indicator

To estimate the site of recording in the tectum, visual receptive field locations (corrected for abnormal eye position; Table 1) were referenced to a tectal map of visual space reconstructed from recordings in normal owls (Knudsen, 1982). For this technique to be valid, the visual map in blind-reared owls must be normal. Three lines of evidence support this conclusion. First, in each electrode penetration, the elevations of visual receptive fields changed systematically from high to low in a nearly linear progression and at a rate predicted by the normal map. Second, in serial penetrations, the azimuths of receptive fields changed with rostrocaudal positioning of the electrode by amounts predicted by the map. Third, 30 recording sites from eight penetrations in two birds (owls 1 and 3) were reconstructed from marking lesions, and all 30 sites were within 500  $\mu\text{m}$  of the anatomical position predicted by the normal map. This degree of precision is indistinguishable from that observed in reconstructions from normal owls.

An example of an electrode tract reconstruction from owl 1 is shown in Figure 3. Note the smooth progression of visual receptive fields (numbered squares) as the electrode penetrated dorsoventrally through the tectum. This pattern was typical of data both from blind-reared and from normal owls.

#### Auditory response properties

The following response properties were first evaluated separately for subpopulations of single units (blind-reared,  $n = 33$ ; normal,  $n = 23$ ) and unit clusters (blind-reared,  $n = 129$ ; normal,  $n = 65$ ) matched for recording location in the rostral half of the tectum. No differences were found between the values for single units and unit clusters, and therefore, the data from single units and unit clusters were combined and are referred to as unit data.

The width and height of auditory best areas (see Materials and Methods) were used as a measure of the sharpness of spatial tuning. All auditory units in blind-reared and normal owls were tuned for source azimuth. The data in Table 3 demonstrate that the sharpness of azimuthal tuning was indistinguishable from that observed in normal owls: mean best-area width was  $18.9^\circ \pm 7.2^\circ$  ( $\pm\text{SD}$ ;  $n = 393$ ) in blind-reared owls and  $18.2^\circ \pm 7.0^\circ$  ( $n = 108$ ) in normal owls. In contrast, unit tuning for elevation tended to be broader in blind-reared owls: mean best-area height was  $39.4^\circ \pm 16.3^\circ$  ( $n = 379$ ) for blind-reared owls versus  $29.5^\circ \pm 12.5^\circ$  ( $n = 108$ ) for normal owls ( $p < 0.0001$ , ANOVA). The mean height of best areas from the blind-reared owls excluded 14 units that responded nearly equally to all elevations (Table 3, Unlimited elevation), a property not seen in the normal owls in this study. Moreover, 10% (40 of 393) of units in blind-reared owls had best areas greater than  $60^\circ$  in height, compared with fewer than 1% (1 of 108) of units sampled from similar portions of the tectum in the normal owls.

The degree to which elevational tuning was degraded varied significantly ( $p < 0.05$ , ANOVA) among the blind-reared birds (Table 3). However, for every blind-reared bird, the mean best-area height was either equal to (two owls) or greater than ( $p < 0.05$ ; five owls) the largest mean height observed among the normal owls (owl 9).

Frequency tuning was typically broad and appeared to be unaffected by blind rearing. In blind-reared owls (1, 2, and 3), CFs ranged from 2.5 to 8.3 kHz, with a median value of 6.2 kHz, and  $Q_{10\text{dB}}$  values (see Materials and Methods) ranged from 0.9 to 7.1, the median value being 2.1 ( $n = 79$ ). In the normal owls, CFs ranged from 1.9 to 8.9 kHz, with a median value of 6.7 kHz, and  $Q_{10\text{dB}}$  values ranged from 0.8 to 5.0, with a median value of 1.7 ( $n = 89$ ).

#### Abnormal auditory space maps

Although the auditory map of space was clearly abnormal in all of the blind-reared owls, each bird's map shared some char-

acteristics with normal maps. First, azimuth was always represented systematically and in the normal orientation: units responding to azimuths near the midsagittal plane (0° Az) were located rostrally in the tectum, and units responding to progressively more contralateral azimuths were located progressively more caudally. Second, elevation was, for the most part, represented systematically (e.g., Fig. 3, numbered circles), though in owls 4 and 6, large portions of the map were reversed in orientation (see below). Third, most units with visual receptive fields in an area directly in front of the animal exhibited essentially normal auditory spatial tuning regardless of the degree of abnormality in the rest of the map.

Topographical abnormalities were assessed in two ways: (1) by measuring the alignment of auditory best areas with visual receptive field locations (visual-auditory alignment), and (2) by observing the regularity in the progression of auditory best areas across the tectum.

**Abnormal visual-auditory alignment.** Because visual receptive field locations were not affected by blind rearing (see above), the alignment of auditory best-area centers with visual receptive field centers of bimodal units provided a means to assess abnormal auditory spatial tuning. As indicated in Figures 4 and 5A–C, visual-auditory alignment in normal owls was excellent. The median size of the alignment errors for all bimodal units from three normal owls was only 2° Az (quartiles, 1–4°;  $n = 106$ ) and 4° El (quartiles, 1–8°). In blind-reared owls, visual-auditory alignment was comparatively poor (Figs. 4, 5D–G). The median size of error for all bimodal units was 5° Az (quartiles, 2–8°;  $n = 332$ ) and 12° El (quartiles, 6–21°;  $n = 318$ ), about three times the normal sizes. Moreover, as will be discussed later, many of the units in the upper quartile had exceptionally large errors. For most units, azimuthal misalignment was smaller than elevational misalignment (Fig. 5D). However, visual-auditory alignment was significantly worse in both dimensions in each of the blind-reared owls than it was in any of the normal owls at the  $p < 0.01$  level (Mann–Whitney  $U$  test,  $z$  distribution). The only exception was elevational alignment in owl 7, in which nearly 50% (6 of 13) of the bimodal units measured were not tuned for sound source elevation (Table 3, Unlimited elevation), which prevented measurement of visual-auditory elevational

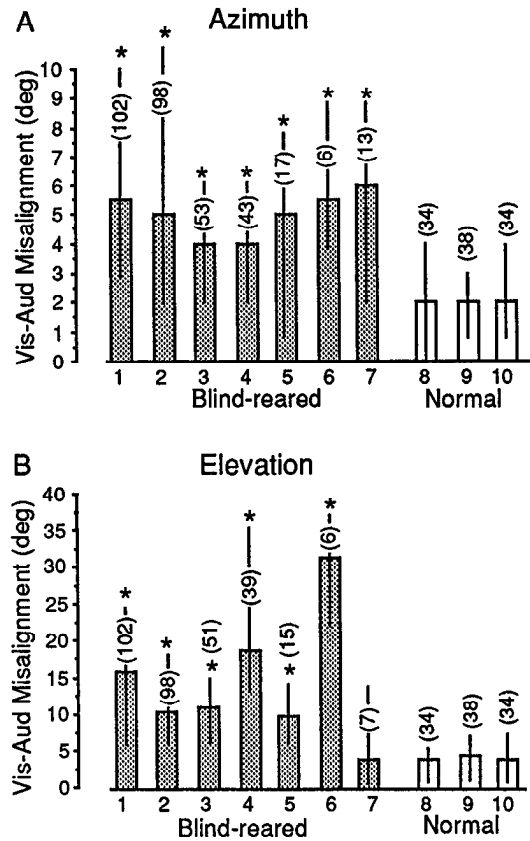


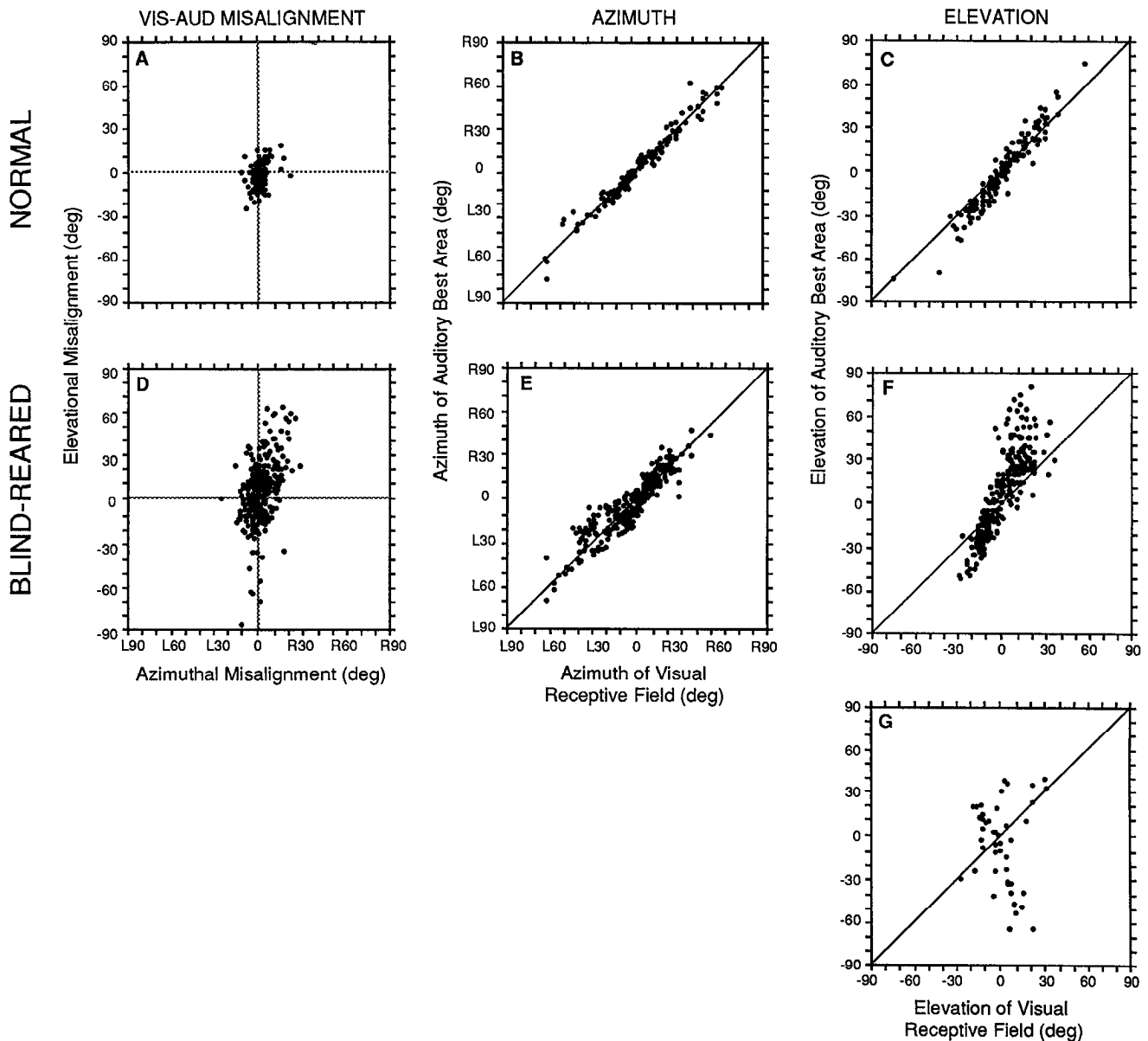
Figure 4. Alignment errors between visual receptive field centers and auditory best-area centers for all bimodal units in each bird. The bars indicate median error magnitudes in azimuth (A) or elevation (B). The vertical lines indicate quartiles. Note that the vertical scales are different in A and B. Sample sizes are in parentheses. An asterisk indicates that the misalignments were significantly larger than those in any of the normal owls ( $p < 0.01$ ,  $z$  values from Mann–Whitney  $U$  tests). Although the elevational misalignments of units shown for owl 7 were not abnormal, 6 of 13 units in this bird were not tuned at all for sound source elevation, a property that was not observed in the normal owls.

Table 3. Size of auditory best areas

Owl	Azimuth (mean ± SD)	Sample size	Elevation (mean ± SD) <sup>a</sup>	Unlimited elevation (no. of units)	Sample size
<b>Blind-reared</b>					
1	19.3 ± 7.5	129	44.7 ± 16.1*	0	129
2	17.8 ± 7.2	116	32.6 ± 12.7	1	115
3	19.9 ± 8.5	71	33.6 ± 14.1	1	70
4	19.1 ± 5.1	41	47.2 ± 19.6*	4	37
5	19.3 ± 5.4	17	45.0 ± 11.1*	2	15
6	15.5 ± 2.1	6	48.0 ± 20.5*	0	6
7	19.8 ± 4.3	13	55.2 ± 18.0*	6	7
<b>Normal</b>					
8	18.1 ± 6.8	32	25.1 ± 10.5	0	32
9	19.5 ± 10.2	31	32.0 ± 12.0	0	31
10	17.4 ± 4.8	45	27.5 ± 10.0	0	45

<sup>a</sup> Best areas that were not bound (unlimited) in elevation are excluded.

\* Significantly larger than normal at the  $p < 0.05$  level (ANOVA).



**Figure 5.** Alignment of auditory best areas with visual receptive fields in all normal (*A–C*) and all blind-reared owls (*D–G*). The plots are based on data from 106 units from normal owls and 332 units from blind-reared owls. In *A* and *D*, visual-auditory misalignments are plotted: each point represents the location of a unit's auditory best-area center relative to the center of its visual receptive field. In *B* and *E*, the azimuths of auditory best-area centers are plotted as a function of visual receptive field centers for all bimodal units. Points that fall on the solid lines (slope of 1) represent units with auditory best areas and visual receptive fields located at the same azimuth. *C*, *F*, and *G* show equivalent data for the elevational alignment of visual and auditory spatial tuning. The data in *G* are from blind-reared owls 4 and 6, in which large portions of the representation of elevation were upside down.

alignments. Thus, in owl 7, elevational tuning was clearly abnormal, as well.

**Map irregularity.** Throughout the tectum in all of the blind-reared birds, the progression of auditory spatial tuning was often erratic (Fig. 6). Figure 7 compares progressions of auditory best areas (solid symbols) recorded in single electrode penetrations in a normal owl (Fig. 7*A*) with those recorded in penetrations in two blind-reared owls (Fig. 7*B,C*). In normal owls, the locations of auditory best areas changed gradually and systematically as an electrode penetrated dorsoventrally through the tectum. In blind-reared owls, the progression of best areas was typically less systematic: best-area azimuths in a single electrode penetration could vary unpredictably over ranges of up to 10°,

and best-area elevations sometimes remained constant over long distances, then jumped abruptly, even as the visual receptive fields (Fig. 7, open symbols) changed in a systematic pattern. Thus, the normally smooth progression of auditory spatial tuning across the tectum was degraded in blind-reared owls.

**Abnormal representations of elevation.** Elevational visual-auditory misalignments were not random across the tectum; nearby units usually had misalignments of similar size and direction even when the misalignments were highly abnormal (Figs. 6; 7*B,C*). In addition, auditory elevational tuning usually progressed across the tectum in one of two abnormal patterns. The first pattern is shown in Figure 6, *A* and *B*. This pattern was the most frequently observed, occurring in owls 1, 2, 3, 5, and 7.



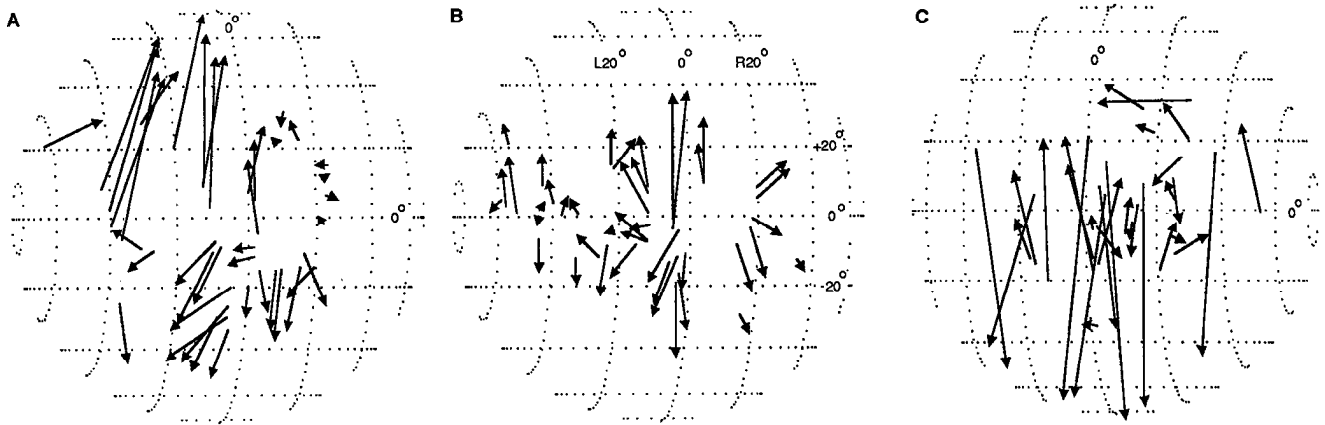


**Figure 6.** Examples of visual-auditory misalignments recorded in three blind-reared owls. Each vector represents the visual-auditory misalignment measured for a single unit; the tail of the vector is located at the center of the visual receptive field, and the head of the vector is located at the center of the auditory best area. The data in *A* are from owl 1; the data in *B* are from owl 3. The misalignments in these birds were similar and represent the most frequently observed pattern. The data in *C*, from owl 4, represent a second pattern characterized by a flipped auditory map of elevation in large portions of the tectum. The plots do not show all of the data from each bird.

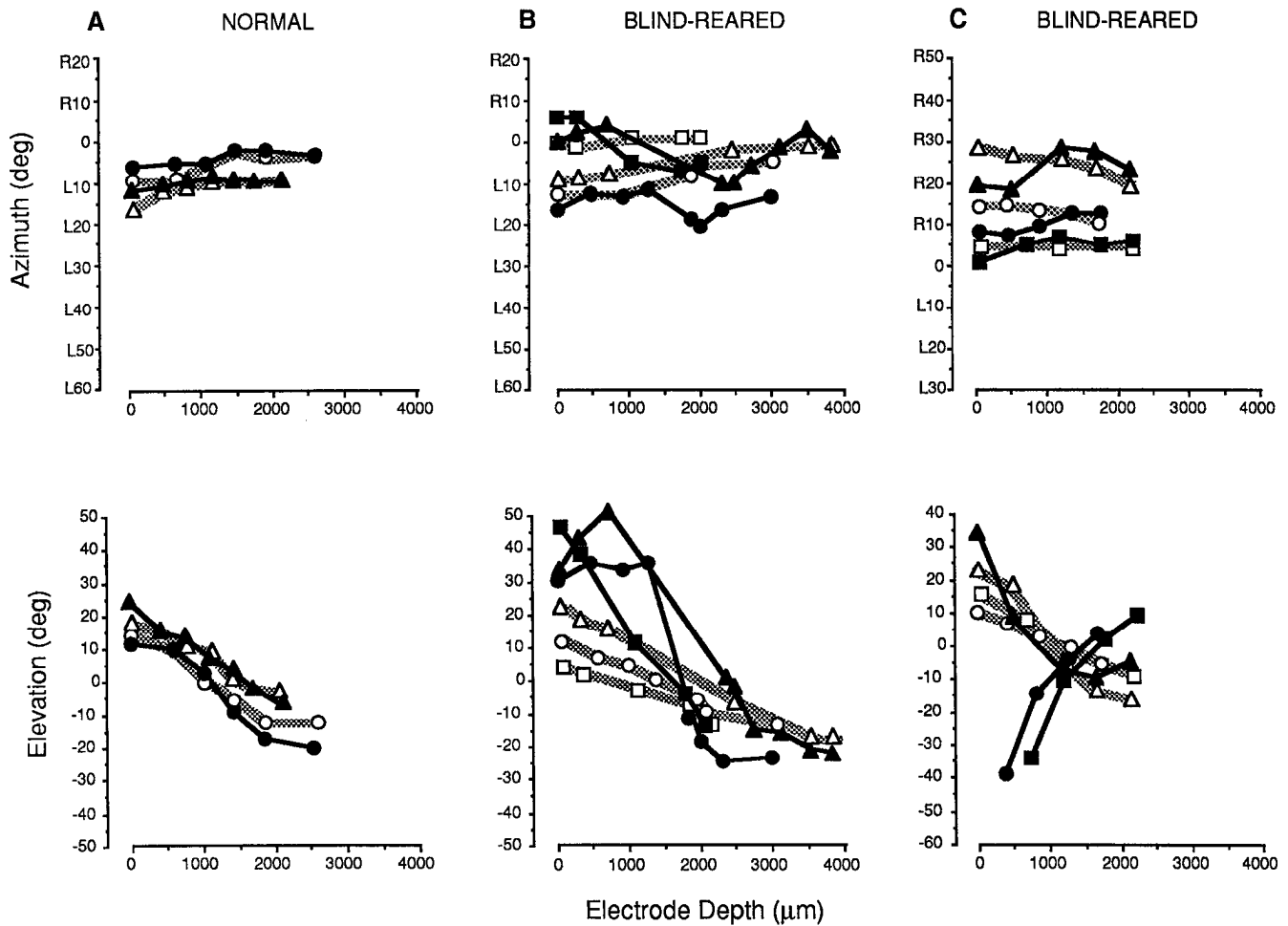


**Figure 7.** Progression of auditory and visual spatial tuning with electrode depth in normal and blind-reared owls. The azimuthal locations (*top row*) and elevational locations (*bottom row*) of visual receptive field centers (*open symbols*) and auditory best-area centers (*solid symbols*) are plotted as a function of dorsoventral electrode depth relative to the depth of the first unit encountered; a given symbol type (*triangle, circle, or square*) indicates data from a single penetration. The data in *A* are from two penetrations in owl 9, the owl with the most erratic auditory map of any normal owl. The data in *B* are from three penetrations in blind-reared owl 1, and those in *C* are from three penetrations in blind-reared owl 4. Note, in *B*, the steeper progression of auditory versus visual elevational tuning and, in *C*, the reversed progression of auditory elevational tuning in two penetrations, indicating a flipped map of elevation in the rostral portion of the tectum. Equivalent symbol types in the upper and lower plots represent data from the same penetration.

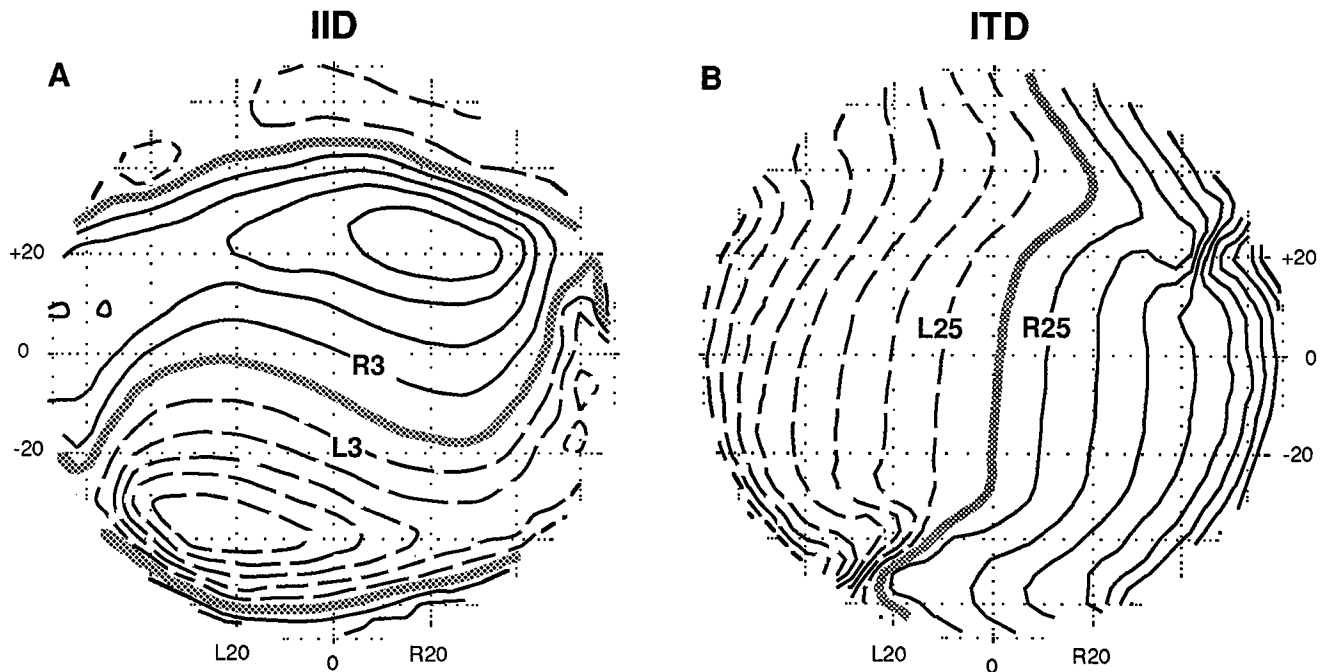


**Figure 8.** Variation of IID (*A*) and ITD (*B*) across the frontal hemifield for the 1/3-octave interval centered near 7 kHz. The plots represent data averaged over the frequency range of 6.3–8.0 kHz measured every 10° in azimuth and elevation from five normal owls. In *A*, contour lines represent isoIID<sub>7kHz</sub> lines in increments of 3 dB; for example, the line labeled R3 indicates those locations for which IID<sub>7kHz</sub> was 3 dB louder in the right ear. Solid lines indicate right-ear-louder; broken lines indicate left-ear-louder. In *B*, contour lines represent isoITD<sub>7kHz</sub> lines in increments of 25 μsec. Solid lines indicate right-ear-leading; broken lines indicate left-ear-leading. The shaded lines indicate IID = 0 dB (*A*) and ITD = 0 μsec (*B*).

Units with visual receptive fields located above  $-10^\circ$  El (dorsal tectum) typically had auditory best areas located higher than visual receptive fields (Fig. 6*A,B*, upward vectors), whereas units with visual receptive fields located below  $-10^\circ$  El (ventral tectum) typically had auditory best areas that were too low (Fig. 6*A,B*, downward vectors). As the electrode passed from the dorsal into the ventral tectum, it encountered units with visual receptive fields located just below the visual plane, between  $-5$  and  $-15^\circ$  El; these units typically had auditory best areas centered at the corresponding elevation (but sometimes at an inappropriate azimuth). Thus, in tecta exhibiting this pattern, the elevations of auditory best-area centers correlated positively with the elevations of visual receptive fields, but the slope of the correlation was greater than 1 (slopes ranged from 1.6 to 1.8 across individuals). We refer to this pattern as a stretched representation.

A second, strikingly different pattern of misalignments was observed in owls 4 and 6 (Figs. 6*C*, 7*C*). Over large portions of the tectum, the auditory representation of elevation was upside-down: many units with high visual receptive fields (dorsal tectum) had best areas located well below the visual plane, and many units with low visual receptive fields (ventral tectum) had auditory best areas located above the visual plane.

The topography of an upside-down representation of elevation was explored adequately only in owl 4 (owl 6 was used primarily for electrical stimulation experiments; see below). As shown in Figure 7*C*, the representation of elevation was flipped in some regions of the tectum, but not in others. In 12 penetrations through the rostral third of the tectum, the progression of elevational tuning was flipped: the locations of auditory best areas began low in dorsal tectum and changed systematically from low to high, even as the visual receptive fields of the same units changed from high to low (e.g., Fig. 7*C*, circles and squares).

Farther caudal in the tectum, the map was oriented normally: in four electrode penetrations, auditory best areas were high in dorsal tectum and low in ventral tectum (e.g., Fig. 7*C*, triangles). Still farther caudal in the tectum, where far contralateral azimuths are represented, the representation of elevation measured in three penetrations was again flipped. As was true in all of the other blind-reared birds, units that had visual receptive fields located at or just below the visual plane tended to have best areas at about the correct elevation (Figs. 5*G*; 7*C*, crossover of shaded and solid lines). Interestingly, though an upside-down representation of elevation was the more unusual pattern among blind-reared birds (2 of 7), this pattern was observed in *both* tecta of owl 4 (only the right tectum of owl 6 was sampled).

To develop some intuition about what these distortions imply in terms of unit tuning for localization cues, we translated the locations of auditory best areas and visual receptive fields into corresponding IID and ITD values using the spatial patterns shown in Figure 8, which are values for the 1/3-octave interval centered near 7 kHz (see Materials and Methods for the assumptions that underlie these translations). [This frequency interval (6.3–8.0 kHz) was chosen because most tectal units respond to frequencies within this range (Knudsen, 1984), and cue values measured over this interval predict the broadband dichotic IID and ITD tuning of tectal units more accurately than values from other intervals (Olsen et al., 1989)]. The elevational tuning of tectal units, and therefore the tectal representation of elevation, is determined in large part by tuning to IID cues (Olsen et al., 1989). As shown in Figure 8*A*, IID<sub>7kHz</sub> is a strongly nonmonotonic function of source elevation: sound is equally intense in the two ears when the source is near  $-10^\circ$  El (shaded lines); IID<sub>7kHz</sub> increases in favor of the right ear as a source ascends, peaks at about 15 dB right-ear louder when the source is at  $+20^\circ$  El, then decreases again to 0 dB as the source ap-

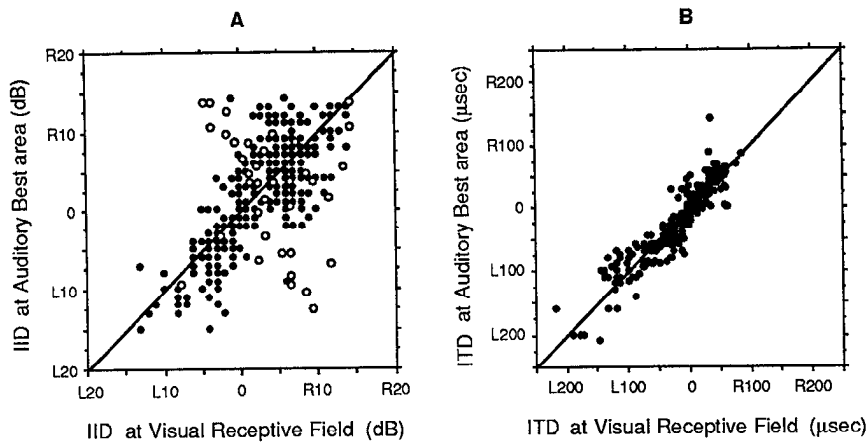


**Figure 9.** Values of  $\text{IID}_{7\text{kHz}}$  and  $\text{ITD}_{7\text{kHz}}$ , corresponding to visual receptive field locations, compared with  $\text{IID}_{7\text{kHz}}$  and  $\text{ITD}_{7\text{kHz}}$  tuning inferred from auditory best-area locations for all units recorded in the blind-reared owls. Values of  $\text{IID}_{7\text{kHz}}$  (A) and  $\text{ITD}_{7\text{kHz}}$  (B) were derived from the spatial patterns shown in Figure 8 (averaged values from five owls over the range of 6.3–8.0 kHz). For units lying along the diagonal lines (slope of 1), cue values based on visual receptive field location and auditory best-area location matched. The open circles in A represent data from owls 4 and 6, in which large portions of the auditory representation of elevation were upside-down.

proaches  $+40^\circ$  El. Similarly,  $\text{IID}_{7\text{kHz}}$  increases in favor of the left ear as a source descends from about  $-10^\circ$  El, peaks at about 17 dB left-ear louder when the source is at  $-40^\circ$  El, then decreases again to 0 dB as the source approaches  $-60^\circ$  El. Below  $-60^\circ$  El, sound is again louder in the right ear.

Because of the highly nonmonotonic relationship between  $\text{IID}_{7\text{kHz}}$  and source elevation, the systematic elevational misalignments observed in the stretched maps (Fig. 5F) do not correspond to a similarly systematic bias in the tuning of units to  $\text{IID}_{7\text{kHz}}$  (Fig. 9A, solid circles). The correlation of  $\text{IID}_{7\text{kHz}}$  values based on visual receptive field centers with  $\text{IID}_{7\text{kHz}}$  values inferred from auditory best-area centers had a slope of 0.97 and an intercept of L0.6 dB ( $r^2 = 0.64$ ). Thus, the stretched representations of elevation did not result from a simple shift in the tuning of units to abnormally large values of  $\text{IID}_{7\text{kHz}}$ .

In contrast, the upside-down representations of elevation clearly predict systematic errors in unit tuning to  $\text{IID}_{7\text{kHz}}$  (Fig. 9A, open circles): units in dorsal tectum should have been tuned to right-ear- rather than left-ear-louder values of  $\text{IID}_{7\text{kHz}}$ , and vice versa for units in the ventral tectum (Fig. 8A). Because a reversal in the organization of IID tuning represents an astonishing change in a fundamental response property, we measured the IID tuning of units directly (using sound delivered through earphones) in the left tectum of owl 4. In the rostral tectum, where the representation of elevation was flipped, the pattern of IID tuning was also reversed relative to normal (three electrode penetrations; 11 units), with units tuned to left-ear-louder IIDs in dorsal tectum and units tuned to right-ear-louder IIDs in ventral tectum (e.g., Fig. 10, penetration 1). Farther caudal in the tectum, where the representation of elevation was oriented normally, units exhibited a normal progression of IID tuning (two electrode penetrations; six units), with dorsal units being tuned to right-ear-louder IIDs and ventral units to left-ear-louder IIDs (e.g., Fig. 10, penetration 2). Thus, blind rearing did indeed allow a reversal, for a large population of units, in the normal progression of IID tuning across the tectum.

**Distorted representation of azimuth.** Azimuthal misalignments between auditory best areas and visual receptive fields were not random across the tectum. There was a tendency for the direction of azimuthal misalignments to correlate with the direction of elevational misalignments (Figs. 5D, 6): when the auditory best area was located above the visual receptive field, it was usually to the right of the visual receptive field (to the right, 115 units; to the left, 59 units), and when it was below the visual receptive field, it was usually to the left (to the left,

75 units; to the right, 38 units). This distortion in the auditory representation of azimuth can be accounted for, in part, by the spatial pattern of ITD cues, which are the primary determinants of unit azimuthal tuning (Olsen et al., 1989). Figure 8B shows how ITDs, measured over a 1/3-octave interval centered near 7 kHz ( $\text{ITD}_{7\text{kHz}}$ ), vary across space. Sound arrives simultaneously at the two ears (Fig. 8B, shaded line) when the source is near the midsagittal plane ( $0^\circ$  Az). As the source moves to the left of  $0^\circ$  Az, sound leads in the left ear by progressively larger amounts up to about 230  $\mu\text{sec}$  left-ear-leading; as the source moves to the right, sound leads in the right ear by progressively larger amounts up to about 230  $\mu\text{sec}$  right-ear-leading. However, the regions that give rise to equivalent values of ITD (Fig. 8B, iso- $\text{ITD}_{7\text{kHz}}$  lines) are not perfectly vertical, but are slanted to the right, similar to the slant of the visual-auditory misalignments (Figs. 5D, 6).

This suggests that, in blind-reared owls, many tectal units could have been tuned correctly for the value of  $\text{ITD}_{7\text{kHz}}$  associated with the locations of their visual receptive fields, despite the misalignments of their auditory and visual receptive fields. This seemed especially likely for units with visual receptive fields located in the upper left quadrant of space, because these units tended to have large visual-auditory misalignments with auditory best areas located consistently above and to the right of visual receptive fields (e.g., Fig. 6A). In this portion of space, iso- $\text{ITD}$  contours also slant steeply to the right (Fig. 8B), consistent with the hypothesis that these units were, in fact, tuned approximately to the values of  $\text{ITD}_{7\text{kHz}}$  associated with the locations of their visual receptive fields.

To test this hypothesis, the locations of auditory best areas and visual receptive fields were translated into corresponding  $\text{ITD}_{7\text{kHz}}$  values using the  $\text{ITD}_{7\text{kHz}}$  spatial pattern (Fig. 8B; see Materials and Methods for assumptions), and the mutual correlation of these  $\text{ITD}_{7\text{kHz}}$  values (Fig. 9B) was compared with the mutual correlation of auditory and visual spatial tuning (Fig. 5E) for the same population of units. The  $\text{ITD}_{7\text{kHz}}$  values predicted by auditory spatial tuning correlated strongly with the values predicted by visual spatial tuning ( $r^2 = 0.88$ ) and with a slope of 0.95 (not significantly different from 1;  $p > 0.05$ ; Fig. 9B). In contrast, the actual azimuths of auditory best-area centers and visual receptive fields correlated with a coefficient of 0.84, but with a slope of 0.88 that was significantly less than 1 ( $p < 0.05$ ). Thus, the location of a unit's visual receptive field predicted its  $\text{ITD}_{7\text{kHz}}$  tuning more reliably than it predicted its azimuthal spatial tuning. This indicates that, for many units,

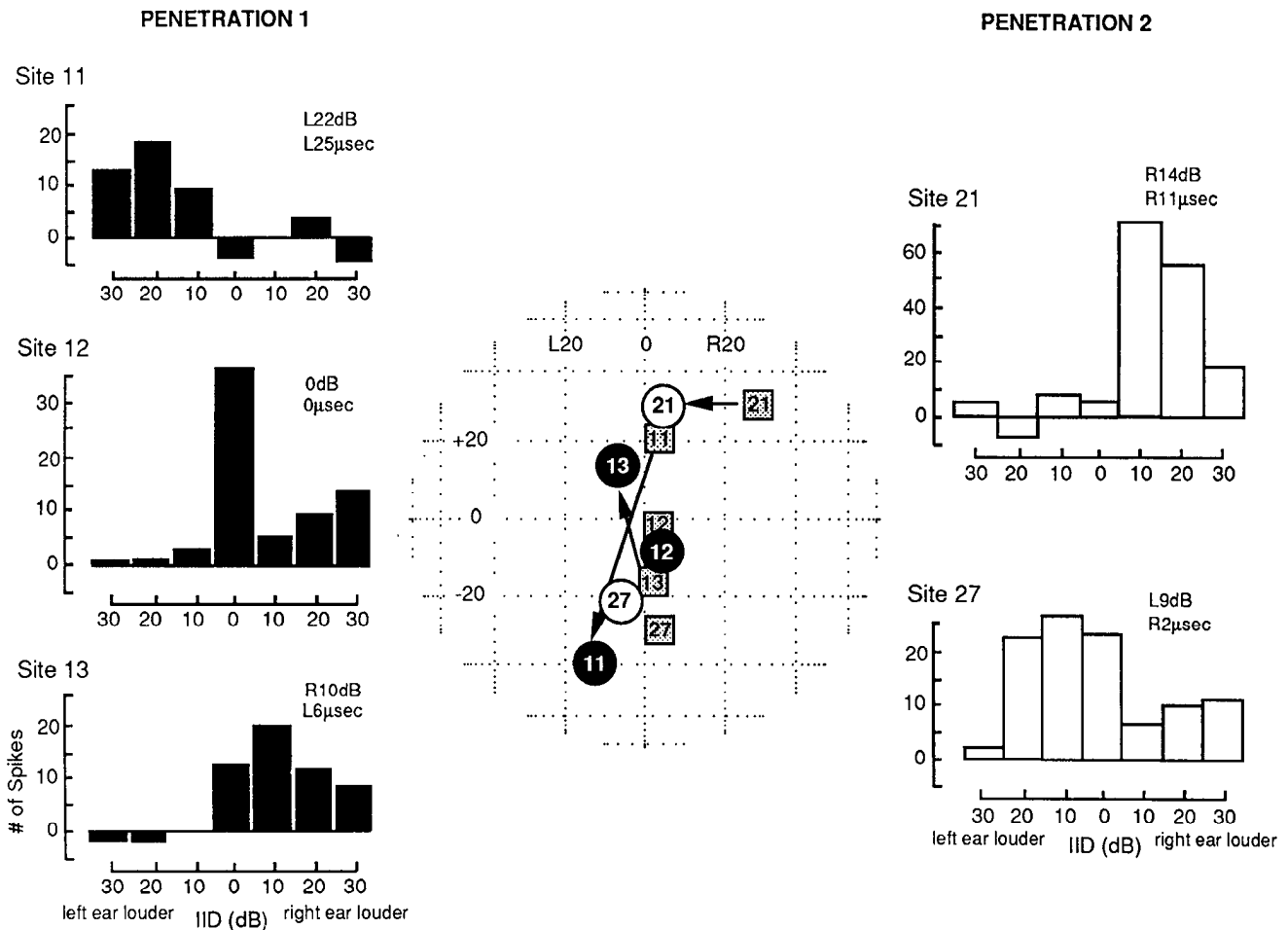


**Figure 10.** IID tuning of units in a flipped auditory map of elevation. The data are from two penetrations in owl 4 in which both free-field spatial tuning (*center plot*) and tuning for dichotically presented IIDs (*histograms*) were measured. *Penetration 1* was made through the rostral portion of the tectum, where the auditory map was flipped; *penetration 2* was made through a more caudal portion of the tectum where the map was oriented normally. Plotted in the *center* are the visual receptive fields (*squares*) and auditory best-area centers (*circles*) for each of the five recording sites. The *numbers* indicate the identity of the recording site; *arrows* link the auditory and visual spatial tuning of individual sites. To the *left* and *right* are histograms showing the tuning at these sites for the IID of noise bursts presented directly to the ears through earphones. Unit responses were summed over 10 presentations of each IID value, and the resting discharge rate was subtracted from these sums. Thus, negative responses indicate activity levels that were below resting levels. The different values of IID were interleaved randomly from trial to trial (see Materials and Methods). The best IID and ITD for each site are indicated on each plot. In *penetration 1* (*sites 11–13*), visual receptive fields descended systematically from high to low (normal pattern), while the auditory best areas of the same units ascended from low to high (abnormal). As predicted by the locations of these best areas, the IID tuning at sites 11 and 13 was opposite in ear preference to that observed at more caudal sites in the same tectum (*sites 21 and 27*), where the map of elevation was oriented normally.

azimuthal misalignment was an indirect result of incorrect tuning for elevation.

The prediction of  $ITD_{7kHz}$  tuning on the basis of visual receptive field location was, nevertheless, less precise ( $p < 0.05$ ) in blind-reared owls ( $r^2 = 0.88$ ) than it was in normal owls ( $r^2 = 0.95$ ). In blind-reared owls, the median difference (absolute value) between the ITDs corresponding with visual receptive fields and those corresponding with the auditory best areas was 15 μsec (quartiles, 5–25;  $n = 307$ ), whereas in normal owls the median difference was only 6 μsec (quartiles, 0–15;  $n = 139$ ). Thus, though blind rearing apparently did not result in systematic distortions of the topography of the ITD map (Olsen et al., 1989), it did appear to degrade the precision of the map.

*Differential degradation of the space map: acoustic basis*

The degree to which the auditory space map was degraded varied across blind-reared animals. However, in all of the animals,

similar portions of the map were consistently more degraded than others. Figure 11 compares the visual receptive field locations of units with visual-auditory misalignments that were relatively small (within the 95th percentile based on the data from the normal owls:  $\leq 10^\circ$  Az,  $\leq 16^\circ$  El) with those of units with visual-auditory misalignments that were unusually large (outside the normal 95th percentile). The distribution of units with large visual-auditory misalignments was not uniform across the map: large azimuthal misalignments clustered in the portions of the map representing locations in the upper left and down and below about  $-10^\circ$  El (Fig. 11A); large elevational misalignments clustered in the portions of the map representing locations above  $0^\circ$  El and below about  $-10^\circ$  El (Fig. 11B). Units with visual receptive fields located between  $0^\circ$  and  $-10^\circ$  El had the lowest probability (see below) of having large visual-auditory misalignments; that is, this portion of the map was degraded relatively little by blind rearing.

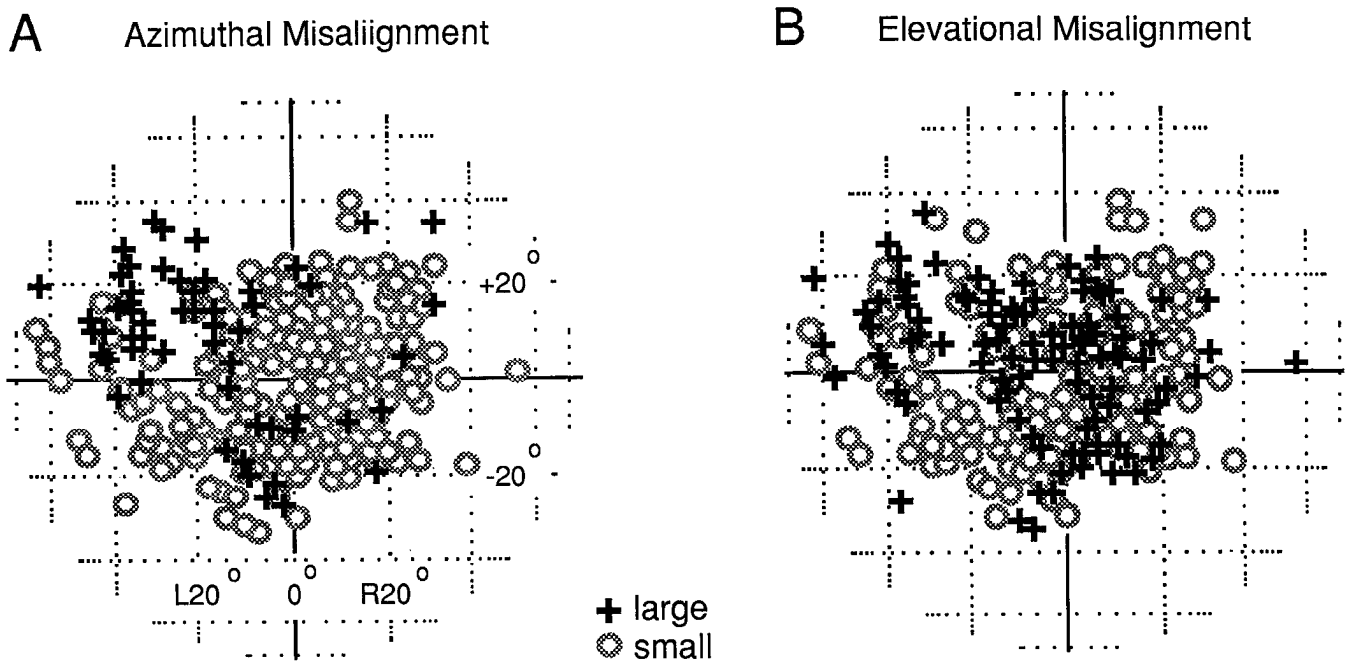


**Figure 11.** Differential degradation of the auditory space map in blind-reared owls. The data illustrate the prevalence of units with large azimuthal (*A*) or elevational (*B*) visual-auditory misalignments in different portions of the map based on visual receptive field locations. Data from all bimodal units in all blind-reared owls are shown. The locations of visual receptive fields of units with large visual-auditory misalignments are indicated by crosses; those having small misalignments are represented by circles. The designation of small versus large misalignments was based on the distribution of misalignment magnitudes measured in normal owls: "large" indicates a misalignment that was beyond the 95th percentile of the normal distribution. The data in *A* are based on azimuthal misalignments greater than  $10^\circ$ ; the data in *B* are based on elevational misalignments greater than  $16^\circ$ .

An acoustic basis for this differential degradation of the space map was sought in the properties of sound localization cues. As mentioned previously, the space map results primarily from systematic changes across the tectum in the tuning of units for IIDs and ITDs (Olsen et al., 1989). Tectal units are broadly tuned for frequency, and for most locations in space, the values of IID and ITD are frequency dependent. The complete set of interaural difference cues produced by a sound source from a given location is described by the interaural difference (IID and ITD) spectra. Two aspects of these spectra were analyzed: (1) the variation of IID or ITD values as a function of frequency, referred to as frequency dependence; and (2) the variation of the spectra across individuals, referred to as individual variability (see Materials and Methods). Figure 12 shows examples of interaural difference spectra from two different locations in space, along with the frequency-dependence and individual-variability values that were calculated from them.

Frequency-dependence values for IID spectra ranged from 0.8 to 8.7 dB across the frontal hemifield. IID spectra were essentially flat (frequency dependence,  $<1.5$  dB) in a narrow region,  $10^\circ$  high and extending  $30^\circ$  to either side, that slanted from the upper right to the lower left across the visual plane (Fig. 13*A*, solid area). Surrounding this region was an area, about  $10^\circ$  wide, in which IID spectra were slightly more complex, with IIDs increasing monotonically as a function of frequency. Beyond this area, and out to the edges of the frontal hemifield, the complexity of IID spectra continued to increase as IIDs began to change nonmonotonically as a function of frequency (e.g., Fig. 12*B*). IID spectra associated with these areas sometimes contained several distinct inflection points between 3 and 9 kHz. The transition from flat to highly frequency-dependent IID spec-

tra could occur rather abruptly, with complexity values changing by up to 3.5 dB with a  $10^\circ$  change in source location.

Frequency-dependence values for ITD spectra ranged from 3 to 35  $\mu$ sec. Relatively flat ITD spectra (frequency dependence,  $<7$   $\mu$ sec) were associated with a much larger region of space than was the case for flat IID spectra (Fig. 13*B*, solid area); this region encompassed the visual receptive fields of most of the units sampled in the map. Flat ITD spectra resulted from sources located between  $+10^\circ$  and  $-20^\circ$  El, and between L20 $^\circ$  and R20 $^\circ$  Az. Beyond this region, the frequency dependence of the ITD spectra increased, with ITD values varying monotonically or nonmonotonically with frequency (Fig. 12*B*).

The individual variability of the IID and ITD spectra exhibited remarkably similar patterns. Both kinds of spectra showed little individual variability over a broad region of frontal space (Fig. 13*C,D*, solid areas). Individual variability increased gradually as the source moved toward the periphery. The differences between the patterns of frequency dependence and individual variability, especially for IID spectra, reflect the fact that sources located outside of the frontal region could give rise to spectra that were complex (highly frequency dependent), but that were nearly identical across individuals.

*Correlation of probability of abnormal alignment with frequency dependence and individual variability of cues.* The distribution of visual receptive field locations sampled in all of the blind-reared birds (bimodal units only) is shown in Figure 11. The visual receptive field locations associated with large misalignments appear particularly related to the pattern of the frequency dependence of IIDs (Fig. 13*A*): large azimuthal and elevational alignment errors are more frequent where IID spectra are complex (cf. Figs. 11, 13*A*). To determine whether this re-

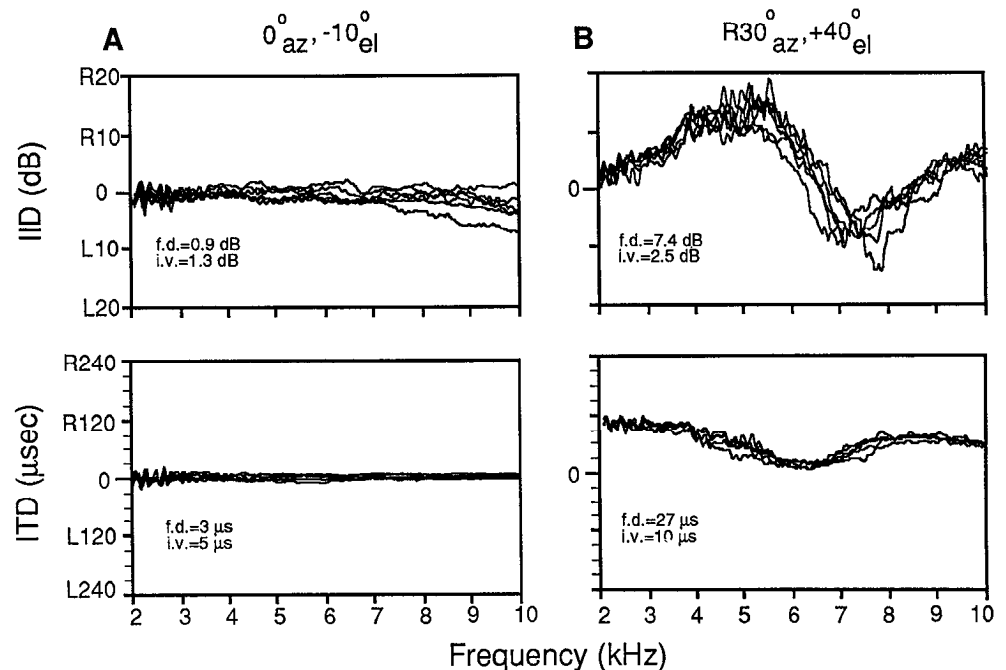


**Figure 12.** Examples of IID spectra (top row) and ITD spectra (bottom row) as recorded in the ear canals with the sound source located at  $0^\circ$  Az,  $-10^\circ$  El (A) or at  $R30^\circ$  Az,  $+40^\circ$  El (B). In each case, spectra are shown from five different owls. The spectra in A are relatively frequency independent and are consistent across owls. In contrast, those in B are highly frequency dependent and relatively variable across owls. Values that quantify the frequency dependence (*f.d.*) and individual variability (*i.v.*), as defined in Materials and Methods, are given for the spectra from each location.

relationship was statistically significant, the following analysis was performed: units were grouped according to the frequency-dependence or individual-variability value associated with the location nearest to each unit's visual receptive field (Fig. 13). Because the data were not evenly distributed across these values, data from units associated with successively larger values of a spectrum property were grouped together until the range contained data from at least 21 units. The value of frequency dependence or individual variability assigned to a given range was the average value among the included units. The number of units within each range with unusually large visual-auditory misalignments (Fig. 14A, data points above the broken line) were compared to the total number of units within that range. (Misalignment sizes themselves were not regressed with the values of cue properties, because the correspondence of cue values with locations is highly nonlinear; i.e., a given change in a unit's cue tuning could lead to misalignments of very different sizes, depending on the region of space.) These ratios revealed the probability of a unit having an abnormally large misalignment in azimuth or elevation as a function of the frequency dependence or individual variability of the IID or ITD spectrum corresponding to the unit's visual receptive field. The correlations of these values were tested to determine whether slopes were significantly different from 0. The results from this analysis are given in Table 4.

The analysis confirmed that the probability of abnormal auditory spatial tuning correlated with the frequency dependence of the IID spectrum associated with the location of the visual receptive field. The most strongly correlated parameters were IID frequency dependence and abnormal elevational tuning (Table 4). Units that had visual receptive fields at locations for which the IID spectrum was flat (frequency dependence,  $<1.5$  dB) had visual-auditory alignments within the normal range in 83% of the cases in the blind-reared birds. In contrast, units that had visual receptive fields at locations for which the IID spectrum was complex (frequency dependence,  $>2.6$  dB) had

only a 50% chance of having alignments within the normal range. The absence of a correlation of ITD spectrum properties with elevational misalignment (Table 4) is consistent with the virtual absence of elevational information in this category of cucs.

The frequency dependence of the IID spectrum correlated strongly with the probability of abnormal azimuthal tuning, as well (Table 4). This correlation reflects, at least in part, the azimuthal misalignment that can result from a large elevational misalignment, even when a unit's ITD tuning matches the ITD value at the unit's visual receptive field (see Distorted representation of azimuth, above). This correlation may also reflect the substantial azimuthal information that is contained in IID spectra, especially in the low-frequency portion of the spectrum (Olsen et al., 1989). The frequency dependence of ITD cues, which are the dominant cues for azimuth, also correlated with the probability of abnormal azimuthal tuning (Table 4).

The individual variability of the difference spectra did not correlate, at the  $p < 0.05$  level, with errors in auditory spatial tuning in either dimension. However, the difference spectra were relatively invariant across individuals over the region of space represented by the sampled units (Fig. 13C,D), making the detection of such a correlation, if one does exist, unlikely.

#### *Alignment of auditory best areas with movement vectors*

To determine whether the abnormalities observed in the auditory space map could be explained by abnormal properties of the tectal motor map, we assayed the motor map in four of the blind-reared birds (owls 4–7). The direction and size of the head movement, or characteristic vector (see Materials and Methods), elicited by microstimulation at 5–15 different sites in each owl were measured and compared with the visual and auditory spatial tuning of units recorded at the same sites (Fig. 15). The motor maps in these birds were abnormal: rarely did a characteristic movement vector correspond with the location of the visual receptive field prior to movement, as it does in normal

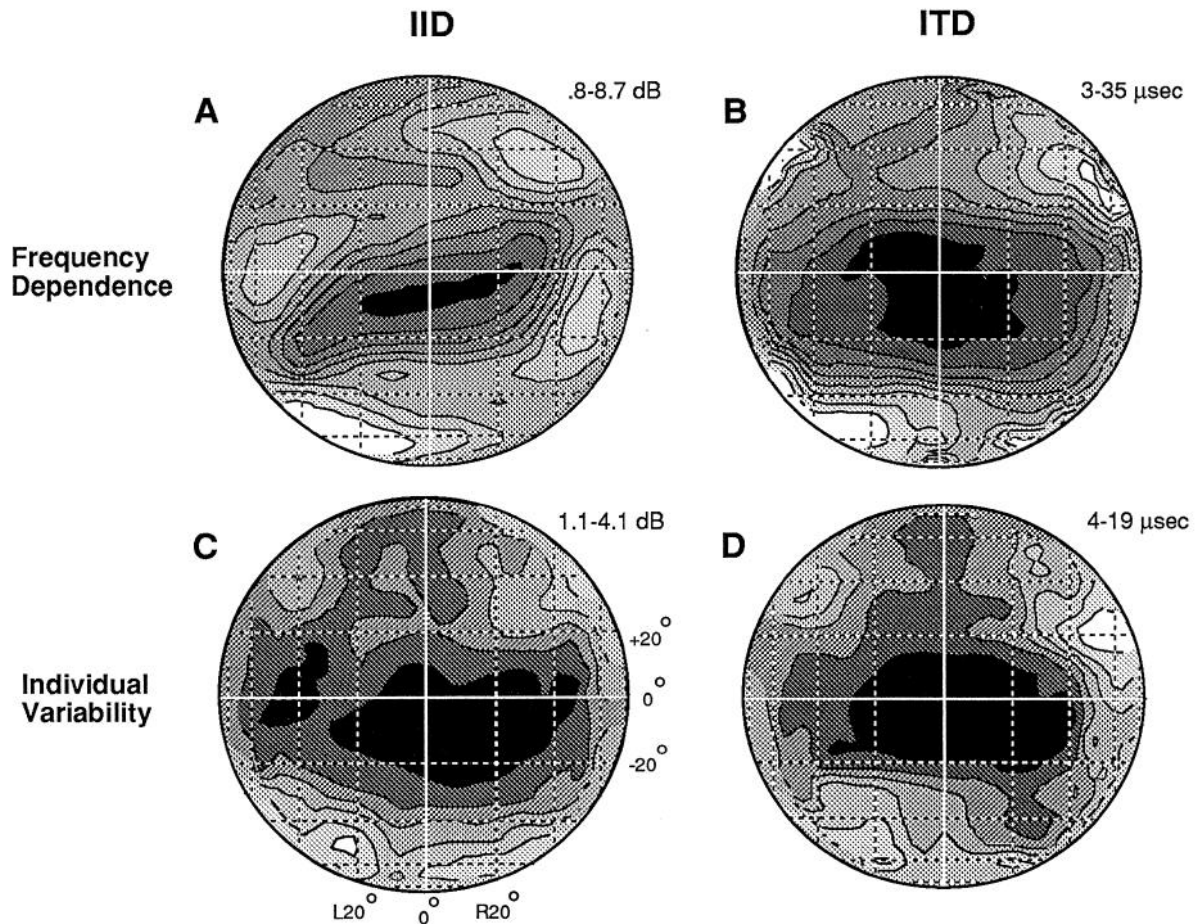


**Figure 13.** Space-dependent variation in the properties of interaural difference spectra. Contour plots indicate the degree of frequency dependence (*A* and *B*) or individual variability (*C* and *D*) of IID (*A* and *C*) or ITD (*B* and *D*) spectra measured across the frontal hemifield in five owls. The contour lines are based on the kinds of data shown in Figure 12. The range of values for each difference spectrum property is indicated at the upper right of each plot. The contour lines represent equal intervals across these ranges, from the minimum (solid areas) to the maximum (open areas) values.

owls (du Lac and Knudsen, 1990). Compared with the location of the visual receptive field, characteristic movements could be too large, too small, and/or misdirected. Figure 15 shows two examples of characteristic vectors (arrows) and the sensory receptive field locations recorded at the sites of stimulation. The data on the left are from owl 7, which had a distorted auditory representation of elevation. The data on the right are from owl 6, which had a flipped auditory representation of elevation (no-

tice that the visual receptive field is above the horizon and the auditory best area is below the horizon).

The data in Figure 16 demonstrate that visual-auditory misalignments and visual-motor misalignments were not related:  $r^2 = 0.03$  for the azimuthal component (Fig. 15*A*) and 0.01 for the elevational component (Fig. 15*B*). This indicates that the abnormal properties of the auditory space map described in the previous section did not result from an adaptation of the au-

**Table 4.** Probability of abnormal visual-auditory alignment correlated with properties of interaural difference spectra

Cue property	Correlation statistics							
	Azimuthal misalignment				Elevation misalignment			
	$r^2$	df	$F$	$p$	$r^2$	df	$F$	$p$
Frequency dependence								
IID	0.68	9	19.2	0.002	0.75	9	24.5	0.001
ITD	0.70	5	9.4	0.04	0.42	5	2.9	0.17
Individual variability								
IID	0.48	7	5.5	0.06	0.33	7	2.9	0.13
ITD	0.46	3	1.7	0.32	0.27	3	0.74	0.48

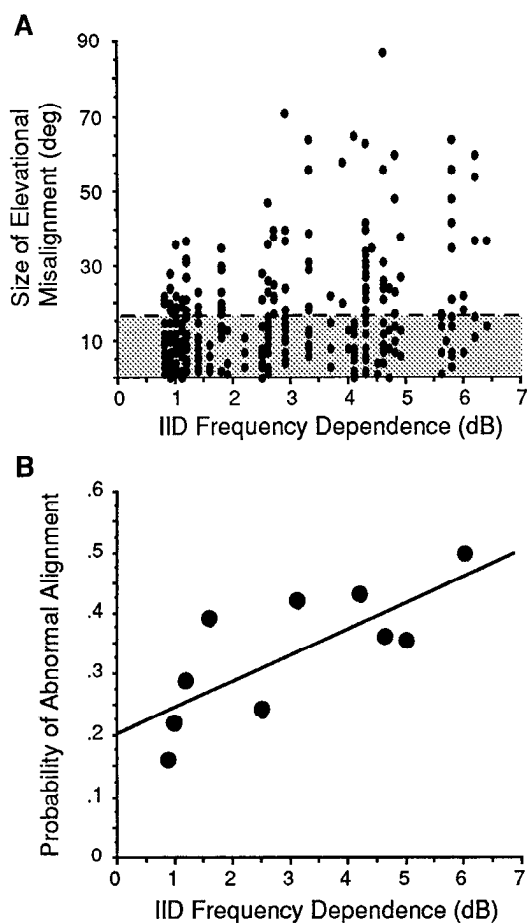


**Figure 14.** Correlation of the probability of abnormal visual-auditory alignment with the frequency dependence of the IID spectrum. These data illustrate how “probability of abnormal alignment” was derived for values of interaural difference spectrum properties that were used in the correlation analyses reported in Table 4. In *A*, the size of a unit’s visual-auditory misalignment in elevation is plotted against the value of the spectrum property (IID frequency dependence) associated with the location of the unit’s visual receptive field. Units were binned into groups of at least 21 based on their associated difference spectrum values. The proportion of units in each group that had unusually large visual-auditory misalignments (outside of the 95th percentile of data from normal owls; *broken line*) was calculated for each restricted range of difference spectrum values and was plotted, in *B*, along the IID frequency-dependence axis according to the average value of all units in the group. The regression line is shown as a solid line. See Table 4 for correlation statistics.

ditary map to the abnormal motor map. Rather, the abnormalities in the auditory and motor maps are separate consequences of blind rearing.

## Discussion

### *Effects of blind rearing on auditory responses in the tectum*

The results demonstrate that an auditory map of space develops in the optic tectum without visual experience. However, the map is far from normal: (1) units in the map tend to habituate, many respond to only one sensory modality, and many are either broadly tuned or lack tuning for source elevation (Table 3); (2) the progression of auditory best areas in both azimuth and elevation is abnormally erratic (Fig. 7), indicating poor map precision; (3) over broad regions of the map, units exhibit systematic errors in spatial tuning (Fig. 6), indicating abnormalities in

the map’s topography; and (4) the representation of elevation may develop in an upside-down orientation (Figs. 6C, 10). In contrast, other aspects of the map in blind-reared owls are remarkably normal: (1) unit tuning for sound source azimuth is sharp (Table 3); (2) best-area locations progress systematically in azimuth and elevation across the tectum (Figs. 3, 6, 7), and the representation of azimuth is oriented normally (Fig. 5E); and (3) the portion of the map that represents the area of space directly in front of the animal is positioned (calibrated) correctly (Fig. 11). These attributes of the space map are thus specified by developmental factors that can operate without vision.

Previous work has shown that early visual deprivation alters auditory responses in the optic tectum (superior colliculus) of several species. Blind rearing increases the proportion of auditory units in the deep tectal layers from 4% to 10% in rats and from 11% to 42% in cats (Vidyasagar, 1978; Rauschecker and Harris, 1983). No comparable increase in the proportion of auditory units was observed in blind-reared barn owls, perhaps because they are already extraordinarily prevalent in normal owls (85%; Knudsen, 1984); the strong auditory representation in the owl may reflect the importance of hearing for this nocturnal predator (Konishi, 1973). In cats, blind rearing leads to the appearance of auditory units in the superficial tectal layers where units are normally exclusively visual (Rauschecker and Harris, 1983). In contrast, superficial layer units in barn owls are normally bimodal (visual and auditory; Knudsen, 1982).

The severity of the effects of early visual deprivation on unit spatial tuning varies across species. In cats, the effects appear to be comparable to those observed in barn owls: qualitative observations indicate that most units in blind-reared cats are still IID sensitive and broadly tuned for frequency, and that auditory receptive fields, though apparently larger than normal, tend to be centered on visual receptive fields (Rauschecker and Harris, 1983). This implies that a map of auditory space does develop, though the topography of the implied map has not been explored. In guinea pigs, the effects of early visual deprivation are considerably more severe: multiunit activity reveals no directional preference for auditory stimuli, and hence a representation of auditory space does not seem to develop at all (Withington-Wray et al., 1989).

The auditory maps in other species that have been studied are based almost exclusively on unit tuning for intensity cues (Hirsch et al., 1985; Palmer and King, 1985; Wise and Irvine, 1985). Intensity cues are highly frequency dependent for all species (e.g., Harrison and Downey, 1970; Knudsen, 1980; Palmer and King, 1985; Middlebrooks et al., 1989; Musicant et al., 1990), and therefore the problems involved in constructing these maps are comparable to those involved in constructing the representation of elevation in the barn owl. Figure 14 and Table 4 demonstrate that elevational tuning errors in barn owls correlate with the frequency dependence of the intensity cues, and we expect that in other species the importance of vision for calibrating different portions of the auditory map may also vary with the frequency dependence of the cues.

### *Effects of blind rearing on sound localization*

The results from the behavioral studies demonstrate that the owl’s capacity to localize sounds develops to a considerable degree without vision. Blind-reared owls localize noise sources, and on average, there is no bias in their localization (Table 2). However, performance is not normal. Blind-reared owls are more difficult to train to orient toward sound sources than are



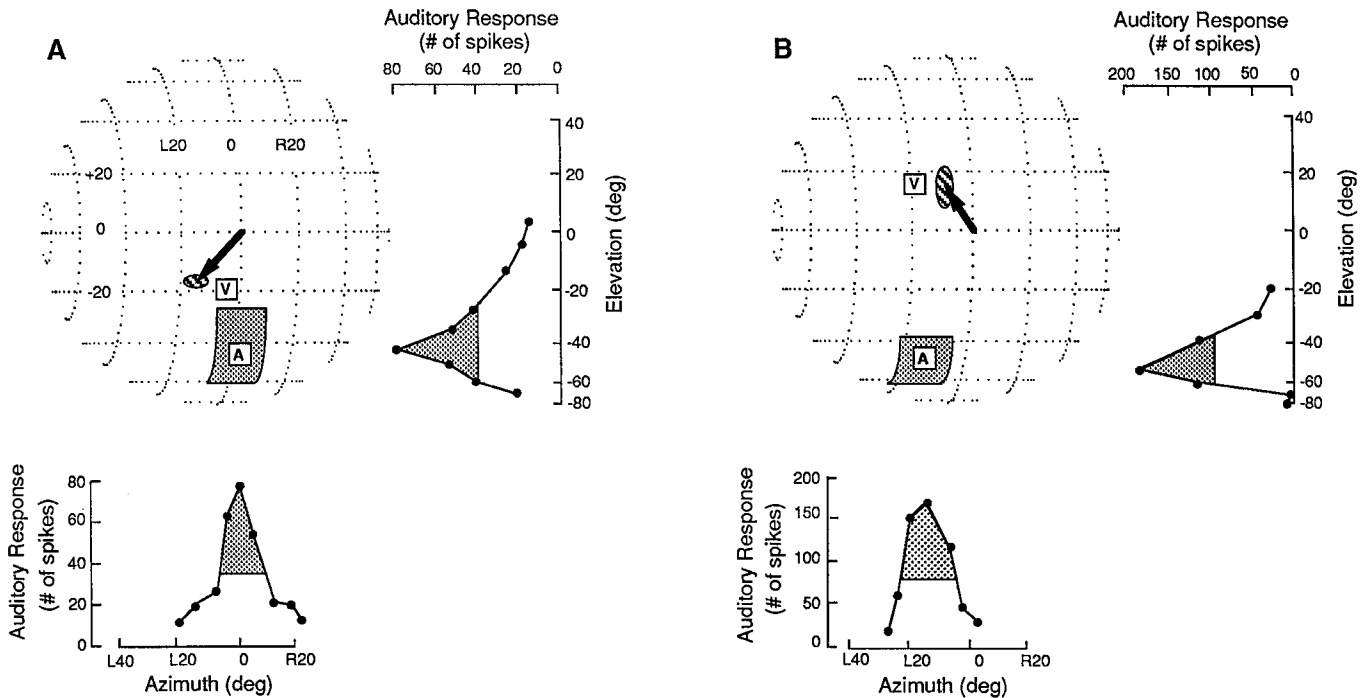


**Figure 15.** Head movements evoked by electrically stimulating the tectum are compared with the visual and auditory receptive fields recorded at the sites of stimulation. The data in *A* are from owl 7; the data in *B* are from owl 6 (which had a flipped auditory map of elevation). The mean size and direction of 10 electrically elicited saccadic head movements are represented by an *arrow*. The range of the elicited movements is indicated by the *hatched ellipse*. Stimulation parameters are given in Materials and Methods. The visual receptive field recorded at the site of stimulation is indicated by an *open square* labeled with a *V*. Below and to the right in each panel are the unit's responses to eight presentations of a noise burst, 20 dB above threshold, with the source positioned as indicated by the data points; azimuth tuning was measured along the units' best elevation, and elevation tuning was measured along the best azimuth. The auditory best area (50% response area) derived from these data is indicated by the *shaded area*. The *open square* labeled with an *A* in each plot indicates the center of the best area.

normal owls, and they never respond with the crispness and reliability of normal owls. Moreover, the variance of the responses is significantly greater than normal both in azimuth and in elevation (Table 2). (It should be remembered here that, with the technique of measuring sound localization we used, both inconsistency in localization and systematic errors associated with specific regions of space can contribute to response variance.) Even with this degradation in performance, sound localization by blind-reared owls is good compared to the normal localization abilities of most other species, with the notable

exception of humans (Makous and Middlebrooks, 1990). Thus, nonvisual sources of information can establish a reasonably good perception of auditory space without vision.

The sound localization performance of blind-reared owls parallel certain characteristics of their auditory space maps. The lack of an overall bias in sound localization (Table 2) is consistent with the symmetry of visual-auditory misalignments in the representation of frontal space (Fig. 5*E,F*). The increase in the variance of localization errors is consistent with the general increase in visual-auditory misalignments (Fig. 5*D*) and the de-

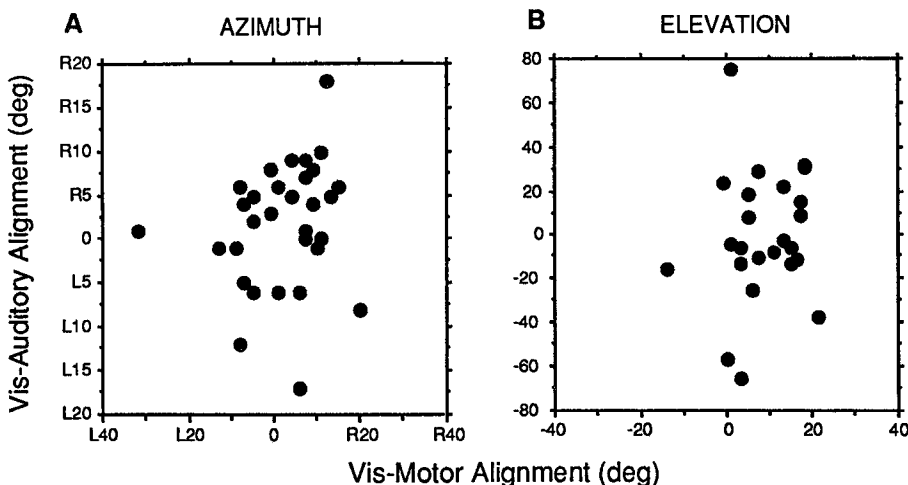


**Figure 16.** In blind-reared owls, visual-auditory alignment errors do not correlate with visual-motor alignment errors measured for the same sites in the tectum. In *A*, the azimuthal component of visual-auditory alignment is plotted as a function of the azimuthal component of visual-motor alignment for 31 different tectal sites from blind-reared owls 4–7. In *B*, the elevational components of the same alignment errors are plotted against each other. Units at some sites were not tuned for sound source elevation, and a visual-auditory discrepancy could not be represented for these sites. Note the change in scale from *A* to *B*. The absence of any correlation in either dimension indicates that abnormal auditory tuning cannot be explained by an adaptation to abnormalities in the motor map.

crease in the precision of the progression of best areas across the map (Fig. 7). The large increase in the variance of the elevational localization errors also corresponds with the increase in the breadth of unit elevational tuning (Table 3), as well as with the large visual-auditory misalignments in elevation (Figs. 5F, 6).

Assuming that properties of the auditory space map are reflected in properties of sound localization behavior in blind-reared owls, the following predictions can be made: (1) because the auditory map is still relatively systematic and the portion of the map representing frontal space is virtually normal, blind-reared owls should exhibit little if any localization deficit in situations where the animal is able to move the head in the sound field and home in on the source, or where it is simply required to make left–right judgments; and (2) the large systematic errors in unit spatial tuning that occur in specific portions of the space map (Fig. 6) should give rise to corresponding localization errors for sources positioned at locations represented by those portions of the map. Thus, the magnitude and direction of localization errors should be both location dependent and variable across individuals.

Given these predictions and the variety of measurement techniques that have been used in previous studies, an interspecific comparison of sound localization by blind-reared animals is difficult. Some studies required categorical responses to sources positioned at regular (predictable) intervals that were large relative to the spatial resolution of the species, some allowed head movements during sound presentation; some required only left–right decisions rather than decisions about absolute location; and most restricted source locations to the horizontal plane. Thus, a finding of no differences between blind-reared and normal animals may reflect inadequacies in the measurement technique. Given these caveats, the following observations can be drawn from the literature: humans that are blind from birth are worse than controls at localizing the absolute locations of sound sources (Fisher, 1964; Jones, 1975), and blind-reared rats are severely impaired in sound localization (Spigelman and Bryden, 1967); in contrast, cats are reported to improve localization accuracy and precision with blind rearing (Rauschecker and Kniepert, 1987). In light of the results from the other species, the results from cats deserve verification.

#### *Importance of vision for different parts of the map*

One portion of the auditory space map is essentially normal in blind-reared owls: the representation of the region of space directly in front of the owl and just below the horizontal plane (Fig. 11). This finding implies that this portion of the map is less dependent on vision than the others. The auditory cues that correspond with sources located in this frontal region are unique in at least four ways: the values of both IID and ITD (1) are near 0 (Fig. 8); (2) are similar across frequency (Figs. 12A, 13A,B); (3) change little through development, even as the head and ears grow; and (4) are the same from one individual to the next (Figs. 12A, 13C,D) and therefore are predictable. In species with symmetrical ears, these properties apply to binaural cues corresponding with sources located along the midsagittal plane (Moore and Irvine, 1979; Middlebrooks et al., 1989; Musicant et al., 1990). The consistency of cue values through development and across generations could permit genetically determined mechanisms to establish connections between neurons coding for 0-dB IID and 0- $\mu$ sec ITD with the representation of frontal space in the tectum. The auditory system might need to calibrate the

lower-level representations of IID and ITD 0 values, but this could be accomplished without vision based on the range of IID and ITD values that an animal experiences; the value of 0 would be the midpoint of this range. Experiments that have investigated the influence of auditory and visual experience on the development of sound localization and the auditory space map have demonstrated an innate predisposition to form normal associations of cue values with locations (Knudsen et al., 1984; Knudsen, 1985; Knudsen and Knudsen, 1986, 1990).

In our analysis of the effects of visual deprivation on the auditory space map, we have ignored the possible influence of monaural cues. The sensitivity of tectal units to monaural cues has not been studied previously. However, most tectal units are driven as strongly as dichotic sounds containing inappropriate monaural cues (constant, flat spectrum) as they are by free-field sounds, and their tuning for IID and ITD spectra predicts reliably their spatial tuning (Esterly and Knudsen, 1989; Olsen et al., 1989). Thus, any influence of monaural cues must be small relative to that of binaural cues.

#### *Rules guiding the development of the auditory map*

*Representation of azimuth.* The reasonably normal representation of azimuth that develops without vision could be generated by a small number of simple developmental rules. This is because the relationship between ITD and azimuth is simple and reliable: ITDs are a monotonic function of source azimuth, and 0- $\mu$ sec ITD corresponds to locations near 0° Az (Fig. 8B). Thus, left-ear-leading ITDs correspond dependably with locations to the left, right-ear-leading ITDs correspond with locations to the right, and maximum ITD values correspond to sources located directly to the side of the head.

Given these relationships and the topographic representation of ITD values within isofrequency laminae at lower levels in the auditory pathway (Sullivan and Konishi, 1986; Wagner et al., 1987; Carr and Konishi, 1990), a few basic rules could underlie the representations of azimuth that were observed in blind-reared owls: (1) in the projections from lower auditory nuclei to the map, neurons tuned to 0- $\mu$ sec ITD at any frequency project to the multimodal representation of 0° Az; this rule accounts for the consistently accurate positioning of auditory 0° Az in the tecta of blind-reared animals (Figs. 5E, 11A). (2) The projections are organized such that contralateral ITDs are represented posteriorly in the tectum. These rules are similar to those established by the molecular mechanisms that guide retinal ganglion cell projections to central visual structures (e.g., Fraser and Hunt, 1980; Whitelaw and Cowan, 1981; Shatz and Sretavan, 1986; Nakamura and O'Leary, 1989). Given these constraints, a systematic progression of azimuthal tuning across the map could develop dynamically as a consequence of Hebbian-like local interactions that cause neighboring neurons to become tuned to similar ITDs together with lateral interactions that cause distant neurons to become tuned to different ITDs (for a discussion of the consequences of local and lateral interactions within maps, see Linsker, 1990); these dynamic processes could also scale the range of ITD tuning to the range experienced by the animal. Alternatively, the progression of azimuthal tuning could result from additional genetic instruction that causes convergent topographic projections to the map from lower-order isofrequency representations of ITD (Wagner et al., 1987). In fact, both of these mechanisms may operate in concert. Note that in either of these scenarios, vision is necessary only for maintaining or refining a preexisting map.

Evidence that a nearly normal map of ITD develops without vision comes from the observation that, in blind-reared owls, a unit's visual receptive field location predicts the ITD corresponding with its auditory best area more accurately than it does the azimuthal location of its best area (Figs. 5E, 9B). This is illustrated by the direction of visual-auditory misalignments (Figs. 5D, 6): when best areas are above visual receptive fields, they also tend to be to the right, and when they are below, they tend to be to the left. This tilt to the visual-auditory misalignments matches the rightward slant of iso-ITD lines (Fig. 8B). The data indicate that units tend to be tuned to approximately the appropriate value of ITD, even when their auditory spatial fields are substantially mislocated as a consequence of inappropriate tuning to other localization cues (presumably IID spectrum; see below).

**Representation of elevation.** It would be more difficult to generate a normal representation of elevation without vision by using similarly simple rules. This is because the rate and pattern of change of IID with elevation are highly frequency dependent. In addition, IID cues can be either monotonic or nonmonotonic functions of elevation depending on frequency (Olsen et al., 1989), and the sign of the IID (right-ear-louder or left-ear-louder) does not always correspond with upper or lower regions of space (Fig. 8A).

The strong frequency dependence of the IID cues results from the dramatic effect that the head and ears have on the intensity of sound reaching the eardrum. At frequencies below 3 kHz, IIDs vary gradually and monotonically with azimuth only. At frequencies between 3 and 5 kHz, the asymmetry of the owl's ears causes IIDs to vary monotonically with both azimuth and elevation, with the gradient of maximal IID change becoming increasingly vertical with frequency (Knudsen, 1980). At frequencies above 5 kHz, IID changes most rapidly as a function of elevation. IID cues in this high-frequency range are thus the most sensitive indicators of sound source elevation, but their patterns are distinctly nonmonotonic (Fig. 8A).

The problem of creating a systematic representation of elevation based on IID cues can be appreciated by considering, as an example, what happens to the IID spectrum as a sound source moves upward from just below the horizontal plane on the left side. At L20° Az, -10° El, a source produces IIDs of about 0 dB at all frequencies, with IIDs of frequencies below 4 kHz slightly favoring the left ear. As the source ascends to +20° El, IIDs of frequencies above 4 kHz favor the right ear by increasing amounts, with the IIDs of frequencies near 8 kHz increasing at about three times the rate of those of frequencies near 4 kHz. By +20° El, IIDs of frequencies greater than 8 kHz have already reached their maximum values. As the source moves farther up, IIDs of these highest frequencies decrease sharply, while IIDs of lower frequencies continue to increase. Above +30° El, high-frequency IIDs favor the left ear, intermediate-frequency IIDs favor the right ear, and low-frequency IIDs favor the left ear. A similarly complicated progression of IID spectra with elevation occurs in other regions of frontal space.

Clearly, a systematic representation of elevation cannot be based on a simple, frequency-independent progression of IID tuning. Instead, IID tuning for low frequencies must progress more slowly across the map than IID tuning for high frequencies. The nonmonotonic relationship between high-frequency IIDs and elevation suggests that a given value of IID may be represented at several locations in the map, and that IID tuning may progress in different directions across the map for different

ranges of frequencies and may reverse direction at various locations in the map, depending on frequency.

The abnormal auditory representations of elevation observed in blind-reared owls suggest constraints that might, nevertheless, influence the development of this map. (1) The consistently accurate positioning of auditory -10° El in the tectum (Figs. 5F,G; 6) implies that neurons in lower auditory nuclei that are tuned to 0-dB IID at any frequency project to the multimodal representation of -10° El. (2) Neighboring neurons in the map tend to exhibit similar elevational tuning errors even though these errors may be otherwise quite unusual (Fig. 6), suggesting the existence of local lateral interactions that cause neighboring neurons to become tuned to similar IID spectra. (3) Even though the topography of the map may be severely distorted or flipped in orientation, a clear tendency persists for elevational tuning to change progressively across the tectum (Figs. 5F,G; 6; 7). This suggests the influence of a second type of lateral interaction within the map (Linsker, 1990) that causes distant neurons to become tuned to different IID spectra. However, the mechanisms that control the development of the map do not rigidly specify its orientation without vision, because the representation of elevation can develop in an upside-down orientation (Figs. 7C, 10). This may reflect the fact that the sign of the IID does not indicate unconditionally whether a sound source is located above or below the animal.

We do not understand the basis of the stretched representation of elevation that was found in most of the blind-reared birds (Figs. 5F; 6A,B). The data presented in Figure 9A (solid circles) show that the stretch of the map did not result simply from a systematic shift in the tuning of units to larger values of IID<sub>7kHz</sub>. Instead, the explanation must include abnormal tuning to IID values of other frequencies within the broad spectral sensitivities of these units. For example, tuning to the entire IID spectrum might progress too rapidly across the tectum, or the spectral sensitivity of units might be shifted downward in frequency while the progression in tuning to IID values across the tectum remains unchanged. Errors in resolving ambiguities in the relationship between IID and source elevation that result from the nonmonotonic patterns of IID (e.g., Fig. 8A) could also contribute to the stretching of the map. Such ad hoc hypotheses can be tested only by direct measurement and comparison of the frequency-specific IID tuning of units in stretched and normal maps.

Vision clearly plays a more critical role in the development of the representation of elevation than it does in the development of the representation of azimuth. Without vision, the representation of elevation may flip upside down, and neurons in portions of the map that normally represent locations associated with highly frequency-dependent IID spectra have an increased probability of becoming tuned incorrectly for space (Fig. 14). We hypothesize that vision shapes the IID tuning of neurons in the map so that each neuron responds to the appropriate set of IID values (corresponding with the location of its visual receptive field), and that this instruction is most crucial when those values vary with frequency.

In animals with symmetrical ears, the correspondence of the sign of the IID with the general direction of the sound source is neither uncertain nor frequency dependent: left-ear-louder IIDs always correspond with locations to the left, and right-ear-louder IIDs always correspond with locations to the right (Harrison and Downey, 1970; Palmer and King, 1985; Middlebrooks et al., 1989; Musicant et al., 1990). Consequently, in such species

the orientation of the IID map could be specified by vision-independent mechanisms that would prevent the IID map from flipping in blind-reared individuals. However, as in barn owls, the spatial patterns of IID cues in all species are highly frequency dependent, being monotonic or nonmonotonic and varying over greater or lesser ranges of IID values, depending on frequency. Thus, based on the results reported here, we would expect auditory space maps that derive primarily from IID tuning to be degraded by early blindness in other species, as well.

#### *Models of visual influence on the auditory map*

In a previous report, three models were put forth to explain the deleterious effects of blind rearing on the auditory space map (Knudsen, 1988). One model proposed that vision is necessary to calibrate the tectal motor map (du Lac and Knudsen, in press) and that the motor map, in turn, shapes the auditory map. In this model, the development of the auditory map is guided by the motor map, without reference to vision. The data presented in Figures 15 and 16 demonstrate that this is not the case: in the absence of vision, the topography of the auditory map does not correspond to that of the motor map. Therefore, this model is no longer tenable.

The other two models remain equally likely. One is that the auditory map is maintained or adjusted by a visual signal that indicates the accuracy of orienting movements toward sound sources. In this model, visual feedback does not occur until the animal has oriented its eyes toward the target. According to this model, visually based error-driven feedback shapes the auditory map. The other model is purely sensory and is based on synchronous activation of visual and auditory inputs. In this model, maintenance or adjustment of the auditory map requires that the animal simultaneously hear and see stimulus sources: synchronous auditory and visual input to a site in the map causes active auditory inputs to that site to be strengthened, while active auditory inputs to other sites are weakened. Which of these models is correct remains to be determined.

#### References

- Carr CE, Konishi M (1990) A circuit for detection of interaural time differences in the brain stem of the barn owl. *J Neurosci* 10:3227–3246.
- du Lac S, Knudsen EI (1990) Neural maps of head movement vector and speed in the optic tectum of the barn owl. *J Neurophysiol* 63:131–149.
- du Lac S, Knudsen EI (in press) Early visual deprivation results in a degraded motor map in the optic tectum of barn owls. *Proc Natl Acad Sci USA*, in press.
- Esterly SD, Knudsen EI (1989) Frequency-dependent tuning for interaural difference cues in space-specific neurons in the owl's optic tectum. *Soc Neurosci Abstr* 15:115.
- Fisher GH (1964) Spatial localization by the blind. *Am J Psychol* 77:2–13.
- Fraser SE, Hunt RK (1980) Retinotectal specificity: models and experiments in search of a mapping function. *Annu Rev Neurosci* 3:319–352.
- Gordon B (1973) Receptive fields in deep layers of cat superior colliculus. *J Neurophysiol* 36:157–178.
- Harrison JM, Downey P (1970) Intensity changes at the ear as a function of the azimuth of a tone source: a comparative study. *J Acoust Soc Am* 47:1509–1519.
- Hirsch JA, Chan JCK, Yin TCT (1985) Responses of neurons in the cat's superior colliculus to acoustic stimuli. I. Monaural and binaural response properties. *J Neurophysiol* 53:726–745.
- Hutchings ME, King AJ, Moore DR (1986) The representation of auditory space in the superior colliculus of ferrets raised with abnormal binaural cues during post-natal development. *J Physiol (Lond)* 381:49P.
- Jones B (1975) Spatial perception in the blind. *J Psychol* 66:461–472.
- King AJ, Hutchings ME (1987) Spatial response properties of acoustically responsive neurons in the superior colliculus of the ferret: a map of auditory space. *J Neurophysiol* 57:596–624.
- King AJ, Palmer AR (1983) Cells responsive to free-field auditory stimuli in guinea-pig superior colliculus: distribution and response properties. *J Physiol (Lond)* 342:361–381.
- King AJ, Hutchings ME, Moore DR, Blakemore C (1988) Developmental plasticity in the visual and auditory representations in the mammalian superior colliculus. *Nature* 332:73–76.
- Knudsen EI (1980) Sound localization in birds. In: *Comparative studies of hearing in vertebrates* (Popper AN, Fay RR, eds), pp 287–322. New York: Springer.
- Knudsen EI (1982) Auditory and visual maps of space in the optic tectum of the owl. *J Neurosci* 2:1177–1194.
- Knudsen EI (1983) Early auditory experience aligns the auditory map of space in the optic tectum of the barn owl. *Science* 222:939–942.
- Knudsen EI (1984) Auditory properties of space-tuned units in the owl's optic tectum. *J Neurophysiol* 52:709–723.
- Knudsen EI (1985) Experience alters the spatial tuning of auditory units in the optic tectum during a sensitive period in the barn owl. *J Neurosci* 5:3094–3109.
- Knudsen EI (1988) Early blindness results in a degraded auditory map of space in the owl's optic tectum. *Proc Natl Acad Sci USA* 85:6211–6214.
- Knudsen EI (1989) Fused binocular vision is required for development of proper eye alignment in barn owls. *Vis Neurosci* 2:35–40.
- Knudsen EI, Knudsen PF (1986) The sensitive period for auditory localization in barn owls is limited by age, not by experience. *J Neurosci* 6:1918–1924.
- Knudsen EI, Knudsen PF (1990) Sensitive and critical periods for visual calibration of sound localization by barn owls. *J Neurosci* 10:222–232.
- Knudsen EI, Blasdel GG, Konishi M (1979) Sound localization by the barn owl measured with the search coil technique. *J Comp Physiol* 133:1–11.
- Knudsen EI, Knudsen PF, Esterly SD (1984) A critical period for the recovery of sound localization accuracy following monaural occlusion in the barn owl. *J Neurosci* 4:1012–1020.
- Konishi M (1973) How the owl tracks its prey. *Am Sci* 61:414–424.
- Kuhn GF (1977) Model for the interaural time differences in the azimuthal plane. *J Acoust Soc Am* 62:157–167.
- Linsker R (1990) Perceptual neural organization: some approaches based on network models and information theory. *Annu Rev Neurosci* 13:257–281.
- Makous JC, Middlebrooks JC (1990) Two-dimensional sound localization by human listeners. *J Acoust Soc Am* 87:2188–2200.
- Middlebrooks JC, Knudsen EI (1984) A neural code for auditory space in the cat's superior colliculus. *J Neurosci* 4:2621–2634.
- Middlebrooks JC, Makous JC, Green DM (1989) Directional sensitivity of sound-pressure levels in the human ear canal. *J Acoust Soc Am* 86:89–108.
- Moore DR, Irvine DRF (1979) A developmental study of the sound pressure transformation by the head of the cat. *Acta Otolaryngol (Stockh)* 87:434–440.
- Musican AD, Chan JCK, Hind JE (1990) Direction-dependent spectral properties of cat external ear: new data and cross-species comparisons. *J Acoust Soc Am* 87:757–777.
- Nakamura H, O'Leary DDM (1989) Inaccuracies in initial growth and arborization of chick retinotectal axons followed by course corrections and axon remodeling to develop topographic order. *J Neurosci* 9:3776–3795.
- Olsen JF, Knudsen EI, Esterly SD (1989) Neural maps of interaural time and intensity differences in the optic tectum of the barn owl. *J Neurosci* 9:2591–2605.
- Palmer AR, King AJ (1985) A monaural space map in the guinea-pig superior colliculus. *Hearing Res* 17:267–280.
- Rauschecker JP, Harris LR (1983) Auditory compensation of the effects of visual deprivation in the cat's superior colliculus. *Exp Brain Res* 50:69–83.
- Rauschecker JP, Kniepert U (1987) Auditory localization behavior in cats deprived of vision. *Soc Neurosci Abstr* 13:871.
- Roth GL, Kochhar RK, Hind JE (1980) Interaural time differences: implications regarding the neurophysiology of sound localization. *J Acoust Soc Am* 68:1643–1651.
- Shatz CJ, Sretavan DW (1986) Interactions between retinal ganglion

- cells during the development of the mammalian visual system. *Annu Rev Neurosci* 9:171-207.
- Sparks DL (1986) Translation of sensory signals into commands for control of saccadic eye movements: role of primate superior colliculus. *Physiol Rev* 66:118-171.
- Spigelman MN, Bryden MP (1967) Effects of early and late blindness on auditory spatial learning in the rat. *Neuropsychologia* 5:267-274.
- Sullivan WE, Konishi M (1986) A neural map of interaural phase difference in the owl's brainstem. *Proc Natl Acad Sci USA* 83:8400-8404.
- Vidyasagar TR (1978) Possible plasticity in the rat superior colliculus. *Nature* 275:140-141.
- Wagner H, Takahashi T, Konishi M (1987) Representation of interaural time difference in the central nucleus of the barn owl's inferior colliculus. *J Neurosci* 7:3105-3116.
- Whitelaw VA, Cowan JD (1981) Specificity and plasticity of retinotectal connections: a computational model. *J Neurosci* 1:1369-1387.
- Wise LZ, Irvine DRF (1985) Topographic organization of interaural intensity difference sensitivity in deep layers of cat superior colliculus: implications for auditory spatial representation. *J Neurophysiol* 54:185-211.
- Withington-Wray DJ, Binns KE, Keating MJ (1989) The maturation of the superior collicular map of auditory space in the guinea pig is disrupted by developmental visual deprivation. *Eur J Neurosci* 2:682-692.